

1 **Mosquito defensins enhance Japanese encephalitis virus infection by facilitating virus**

2 **adsorption and entry within mosquito**

3 **Running title: Mosquito defensins increase JEV transmission potential**

4

5 Ke Liu¹, Changguang Xiao¹, Shumin Xi¹, Muddassar hameed¹, Abdul Wahaab¹, Donghua Shao¹,

6 Zongjie Li¹, Beibei Li¹, Jianchao Wei¹, Yafeng Qiu¹, Denian Miao³, Huaimin Zhu^{2*}, Zhiyong Ma^{1*}

7

8 ¹ Shanghai Veterinary Research Institute, Chinese Academy of Agricultural Science, No. 518, Ziyue

9 Road, Shanghai 200241, P.R. China, ² Department of Pathogen Biology. Second Military Medical

10 University. Shanghai, 200433, P.R. China, ³ Institute of Animal Husbandry and Veterinary Science,

11 Shanghai Academy of Agricultural Sciences, Shanghai 201106, PR China

12 * Correspondence: zhiyongma@shvri.ac.cn

13

14

15

16

17 **Abstract**

18 Japanese encephalitis virus (JEV) is a viral zoonosis which can cause viral encephalitis, death
19 and disability. *Culex* is the main vector of JEV, but little is known about JEV transmission by
20 this kind of mosquito. Here, we found that mosquito defensin facilitated the adsorption of
21 JEV on target cells via both direct and indirect pathways. Mosquito defensin bound the ED III
22 domain of viral E protein and directly mediated efficient virus adsorption on the target cell
23 surface, Lipoprotein receptor-related protein 2 expressed on the cell surface is the receptor
24 affecting defensin dependent adsorption. Mosquito defensin also indirectly down-regulated
25 the expression of an antiviral protein, HSC70B. As a result, mosquito defensin enhances JEV
26 infection in salivary gland while increasing the possibility of viral transmission by mosquito.
27 These findings demonstrate that the novel effects of mosquito defensin in JEV infection and
28 the mechanisms through which the virus exploits mosquito defensin for infection and
29 transmission.

30

31

32

33 **Introduction**

34 Japanese encephalitis virus (JEV), a member of *Flaviviridae flavivirus*, is prevalent in
35 Asia-Pacific tropical and subtropical regions [1-3]. JEV is mainly transmitted through
36 mosquito bites [2, 4]. Pigs are reservoir hosts for JEV, and humans, horses and other animals
37 are dead-end hosts [2, 5]. Because the prevention and control of JEV rely on vaccines with a
38 limited window of protection [6-8], JEV can easily cause death or permanent disability. More
39 than 100,000 people are at risk of JEV infection, and immunocompromised children and older
40 individuals are at particular risk [9, 10]. The World Health Organization has reported that
41 more than 67,900 cases of JEV infection globally each year, more than 10,000 of which are
42 fatal. As global temperature increases, the clinical incidence of Japanese encephalitis is
43 increasing as well, owing to an increase in the habitat range and activity of mosquitoes
44 carrying JEV as the climate warms [2, 4, 9]. Few studies have addressed the transmission
45 mechanism of JEV by mosquito vectors [4]. Thus, a detailed understanding of the interaction
46 between JEV and mosquito vectors will be essential to improve control of JEV transmission.

47 *Culex* is the principal vector of JEV [11, 12]. The virus can spread throughout the
48 mosquito body, including salivary glands [13]. When an infected mosquito bites humans or

49 animals, the virus is transmitted to the skin through the saliva. The mosquito vector also
50 induces an immune response to JEV [14-16]. For example, C-type lectin and a series of
51 proteins increase rapidly after infection [17, 18]. C-type lectin plays an important role in
52 infection by JEV and other *Flaviviridae* viruses in mosquitoes, but the role of defensin has
53 not yet been clearly characterized.

54 Defensins are antimicrobial peptides consisting of 25–60 amino acids that are produced
55 by innate immune system [15, 19]. Defensin is one of the crucial immune effectors in insects
56 [20]. The antiviral effects of defensins have been well described in mammalian cells. Human
57 defensins have been reported to inhibit herpes simplex virus type 2 (retrocyclin-1,
58 retrocyclin-2) [21], human immunodeficiency virus (human beta defensin-1, human beta
59 defensin-2, Human beta defensin-3) [22, 23] and other viruses. However, human beta
60 defensin-6, expressed by adenovirus vectors, enhances parainfluenza virus type 3 replication
61 [24]. Normally, mammalian defensins can directly destroy the virus particles by binding to
62 the surface of envelope protein. They can also interact to the cell surface receptor and
63 influence cell signal transduction [19, 25]. Although there are many differences between the
64 mammalian and mosquito immune systems, defensins are considered important effectors in

65 the mosquito immune response. Therefore, the role of mosquito defensins during the process
66 of JEV infection requires further study.

67 In this study, we observed complex roles of mosquito defensin in JEV infection: a weak
68 antiviral effect and a strong effect enhancing binding. In the latter, defensin directly binds the
69 ED III domain of the viral E protein and promotes the adsorption of JEV to target cells by
70 interacting with lipoprotein receptor-related protein 2 (LRP2), thus accelerating virus entry.
71 Mosquito defensin also down-regulates the expression of the antiviral protein HSC70B on the
72 cell surface, thus facilitating virus adsorption. Together, our results indicate that the
73 facilitation effect of mosquito defensin plays an important role in JEV infection and potential
74 transmission.

75

76 **Results**

77 **JEV infection up-regulates defensin expression *in vivo* and *in vitro***

78 Defensin is one of the major innate immunity effectors in mosquitoes. To study the role
79 of defensin in JEV infection, we first assessed the expression of defensin in *Culex pipiens*
80 *pallens* (*Cpp*) which is the natural vector of JEV after infection. Five-day-old female

81 mosquitoes after emergence were infected by a microinjector with a dose of 1000 MID₅₀ [18].

82 The mosquitoes were collected 4, 7 and 10 days after injection, and the JEV E mRNA levels

83 in the whole body, salivary gland and midgut were determined. JEV E mRNA showed higher

84 levels in the salivary gland than in the whole body and midgut (Fig. 1A). At 10 days, the JEV

85 E mRNA level increased dramatically, thus indicating that the virus reproduced rapidly

86 during this period. For instance, JEV E mRNA levels increased by 9.7- and 11.7-fold at 10

87 days compared with 7 days in the whole body and midgut, respectively. A greater increase

88 was observed in the salivary gland, reaching 14.9 fold at 10 days compared with 7 days.

89 Because high virus levels in mosquitoes were observed 7 and 10 days post JEV infection, we

90 then determined the defensin A and total defensins mRNA level in the whole body on 7 and

91 10 days. *Cpp* defensin A mRNA levels on both days were significantly higher in the JEV

92 infection group than the control group, although the level decreased slightly at 10 days (Fig.

93 1B). Change levels of total defensins showed the similar trend (Fig. 1B). Furthermore, we

94 compared *cpp* defensin A and total defensins mRNA levels in the whole body, salivary gland

95 and midgut. Defensin A and total defensins mRNA showed similar levels of up-regulation in

96 the salivary gland and whole body, which were higher than those in the midgut (Fig. 1C).

97 Significantly higher mRNA levels ($p < 0.005$) were observed in the JEV infection group than
98 the control group for whole body, salivary and midgut. This suggested that *Cpp* defensin A
99 expression was positive correlated with JEV infection in mosquitoes.

100 The gene encoding *cpp* defensin was not found in the NCBI database. According to
101 PCR amplification (Fig. S1A), sequencing and BLASTn (<https://blast.ncbi.nlm.nih.gov>)
102 results, we found two gene types of defensin: defensin A (submitted to NCBI with accession
103 number MH756645) and an incomplete information defensin. The mature protein regions of
104 these two defensins shared 99.5% sequence similarity (Fig. S1B). We designed specific
105 primers (Table. S1, Fig. S2) for real-time PCR detection according to the *Cpp* defensin A
106 sequence. However, no specific primers were available for the unnamed defensin, because
107 scarce specific sequence was obtained. Therefore, we quantified the mRNA copy number of
108 total and type A defensins to determine which subtype is the primary defensin in *cpp* (Fig.
109 S1C). The fold change of mRNA levels of defensin A were significantly higher (7 days,
110 $p < 0.05$) than or similar (10 days) to the total defensin levels (Fig. 1B), thus it implied that
111 defensin A accounts for the majority of total defensins. To analyze whether defensin
112 functioned universally among organisms, we aligned the defensin protein sequences of

113 mosquito vectors of flavivirus. We also quantified the mRNA copy number of total and type
114 C defensins to determine which subtype is the primary defensin in *Aedes albopictus* (*aa*) (Fig.
115 S1C). *Aedes* defensin C is the major type of defensin in C6/36 cell, a cell line from *Aedes*
116 *albopictus*. The sequence similarities were all above 97.6% between mosquito vectors (Fig.
117 S1D), suggesting that mosquito defensins serve similar functions. In contrast, the sequence
118 similarities were significantly low between mosquitoes and human (Fig. S1E). We then used
119 *cpp* defensin A (accession number MH756645) and *aa* defensin C (accession number
120 XP_019527114.1) to study the functions of defensin in JEV infection within mosquito
121 vectors.

122 To confirm the up-regulation of defensin in different mosquito vectors caused by JEV
123 infection, we infected C6/36 cells with JEV *in vitro*. JEV E mRNA levels increased from 24 h
124 to 120 h post JEV infection (Fig. 1D). We further analyzed the change of total defensins and
125 primary defensin (*aa* defensin C, Fig. S1C) after JEV infection. *aa* defensin C mRNA levels
126 were up-regulated to 2.75-, 11.9-, 19.7-fold in JEV infection compared with mock infection at
127 1, 3 and 5 days, respectively (Fig. 1E). Also total defensins were up-regulated after JEV
128 infection (Fig. 1E). Together, our results indicated that defensin levels were up-regulated after

129 both *in vivo* and *in vitro* infections.

130

131 **Mosquito defensin shows species specificity in facilitating JEV infection**

132 Mature defensin is an extracellular protein which length is less than 60 amino acids. To

133 confirm the function of defensin on JEV infection, we synthesized mature defensin peptides

134 with high purity ($\geq 99\%$) to perform further analysis. Scrambled defensin peptides were used

135 as controls. *Cpp* defensin A and *aa* defensin C peptides were used in both *in vivo* and *in vitro*

136 experiment. Defensins and JEV were pre-mixed before injection into mosquitoes.

137 Unexpectedly, in *in vivo* experiment, JEV E mRNA levels increased by 2.95- and 6.13-fold in

138 the *cpp* defensin A treated groups compared with the control groups at 7 and 10 days post

139 infection, respectively (Fig. 2A). And the same changing trend of JEV level was observed in

140 *aa* defensin C treated group (Fig. 2A). We also confirmed this enhancement of defensins on

141 JEV infection by RNA interference. siRNA sequences target *Cpp* defensins or *Cpp* defensins

142 A were designed and used in *in vivo* RNA interference. JEV E mRNA levels were decreased

143 by more than 5 fold in *Cpp* defensin siRNA groups and more than 3 fold in *Cpp* defensin A

144 siRNA groups compared to scramble group (Fig. 2B, Fig. S3A). Indirect immunofluorescence

145 assay (IFA) analysis also showed higher JEV E levels in the mosquito defensin treated cells
146 than the control (Fig. 2C), and lower JEV E levels in the mosquito defensin knockdowned
147 cells than the control (Fig. 2C).

148 To compare the role of defensin from different species, human defensin β 2 showed high
149 antiviral activity was synthesized [25, 26]. Firstly, we compared the effects of *aa* defensin C,
150 *Cpp* defensin A and human defensin β 2 on C6/36 cells. *aa* defensin C enhanced JEV infection
151 on C6/36, as indicated by both JEV E mRNA (4.88 fold) and TCID₅₀ (1.3 titer) levels (Fig.
152 2D i and ii). Treating with *Cpp* defensin A also resulted in the enhancement of JEV
153 infection. In contrast, human defensin β 2 inhibited JEV replication on C6/36 cell, thus
154 demonstrating that defensins from different species have diverse functions in JEV infection
155 (Fig. 2D i and ii). To confirm this effect of mosquito defensin, we used siRNAs target
156 defensin of C6/36. JEV was inoculated and detected after siRNAs transfection. JEV E mRNA
157 levels decreased by 4.7 to 6 folds in *aa* defensin interference groups, and decreased by 2.3 to
158 3.1 folds in *aa* defensin C interference groups respectively (Fig. 2E i and ii, Fig. S3B). These
159 results were consistent with the *in vivo* data.

160 To obtain detailed insight into the function of mosquito defensin, we analyzed the effects

161 of mosquito defensin on mammalian cells contain Vero and BHK-21. *aa* defensin C reduced
162 the JEV replication by 2.2 to 2.7 folds (Fig. 2F i and Fig. 2G i) and decreased JEV TCID₅₀
163 levels by 0.6 to 0.8 titers (Fig. 2F ii and Fig. 2G ii), thus indicating that it inhibits JEV
164 infection in mammalian cells as human defensin dose. Although the inhibition ability of *aa*
165 defensin C was lower than that of human defensin β 2, it still inhibited JEV replication.
166 Therefore, the facilitation effects of mosquito defensin on JEV were valid only on mosquitoes
167 and mosquito cells. To confirm that the effect of defensins was not due to cytotoxicity, we
168 measured the IC₅₀ of each defensin through MTT assays. The results showed that defensins
169 had no significant cytotoxicity on cells (Table. S2).

170

171 **Mosquito defensin enhances JEV adsorption to target cells**

172 To study the exact mechanisms of mosquito defensin facilitates JEV infection, we
173 analyzed the influence of *aa* defensin C on different infection steps on C6/36 cell. As
174 infection steps can be measured by temperature and time shift, we detected adsorption,
175 uncoating and replication of JEV [27]. Adsorption was determined to be a key step in the
176 facilitation effect (Fig 3A). Next, we detected JEV adsorption at different time points. JEV

177 mixed with defensin or scrambled peptides was inoculated to C6/36 cells for different time
178 points at 0°C. After being washed with PBS for three times, cells with absorbed JEV were
179 collected. JEV E mRNA levels were determined by real-time PCR. C6/36 cells treated with
180 *aa* defensin C showed significantly higher JEV E mRNA levels at 4 and 6 h post adsorption,
181 proof that defensin enhanced JEV adsorption to C6/36 (Fig. 3B). IFA showed that JEV
182 adsorption greatly increased in a time course of *aa* defensin C treatment (Fig. 3C and Fig.
183 3D). Both nuclear staining (DAPI) and membrane staining (Did) of C6/36 cell were
184 conducted in IFA adsorption analysis. There was stronger JEV adsorption in the *aa* defensin
185 C groups than the control groups at each time points in both DAPI staining (Fig. 3C) and Did
186 staining (Fig. 3D) cells. To study how mosquito defensin facilitated JEV adsorption, FITC
187 labeled *aa* defensin C was used. Defensin-FITC and JEV were mixed before incubation at
188 0°C. After incubation, unabsorbed defensin and JEV were washed by PBS for five times. The
189 cells were collected at the indicated time points to observe the co-localization of defensin and
190 JEV. Strong co-localization on the cell surface was observed between *aa* defensin C and JEV
191 (Fig. 3E) and increased over time. Thus, the facilitation effect of mosquito defensin on JEV
192 was attributed to the binding between them. Additionally, JEV mixed with *cpp* defensin A

193 showed high adsorption capacity in salivary glands (Fig. 3F). Take together, our results
194 indicated that mosquito defensin is able to bind JEV and facilitate virus adsorption.

195 The interaction between defensin and JEV was also confirmed by ELISA. The plate
196 wells were coated with *aa* defensin C, incubated with JEV and next incubated with anti-JEV
197 antibody. As expected, JEV bound defensin efficiently. Even with a 250 ng defensin coating
198 treatment, the JEV level was significantly higher than that in the control group (Fig. 3G). To
199 determine the adsorption capacity of the JEV-defensin complex to C6/36 cells, we coated
200 plate wells with fresh C6/36 cells after polylysine treatment, added pre-mixed defensin and
201 JEV, and detected JEV with anti-JEV monoclonal antibody. In accordance with the results of
202 qPCR and IFA, the interaction of defensin with JEV significantly enhanced JEV adsorption to
203 C6/36 cells (Fig. 3H).

204 Based on the previous results, we deduced that mosquito defensin can efficiently bind to
205 cell surface. The interaction of mosquito defensin with the cell surface was assessed through
206 ELISA. Defensin directly interacted with C6/36, and a higher FITC value than that of the
207 control was observed (Fig. 3I). This finding implied that the facilitation effect of defensin on
208 JEV was caused by increasing the affinity of JEV on the cell surface.

209

210 **Defensin directly binds the JEV ED III domain**

211 Defensins can bind to viral envelope protein [25]. To precisely understand the interaction
212 mechanisms of JEV enhancement mediated by defensin, we expressed the three structural
213 proteins (C, prM and E) of JEV and the exposure area (ED III) of E protein through an S2
214 insect protein expression system [28, 29], and further purified these proteins via 6×His
215 agarose. To analyze the interaction between viral proteins and defensins, two ELISA methods
216 were used. The plate wells were coated with defensin, incubated with purified proteins and
217 detected by corresponding antibodies. Scrambled defensin was used as control. Absorbance
218 results showed high affinity between *aa* defensin C and E protein or ED III protein, which
219 were ~0.95 and ~1.17, respectively (Fig. 4A). Consistent results were observed in
220 defensin-FITC testing. The plate wells were coated with purified viral proteins and then
221 incubated with *aa* defensin C-FITC or scrambled defensin-FITC. E and ED III proteins
222 showed higher fluorescence values of 332 and 369, respectively (Fig. 4B). Both tests
223 suggested that the ED III domain of E protein is the key region involved in *aa* defensin C and
224 JEV binding. Subsequently, purified E and ED III proteins were mixed with *aa* defensin C

225 and used to inoculate C6/36 cells at 0°C for 4 h. Unabsorbed defensin and JEV were removed
226 by washing with PBS after incubation. The effect of *aa* defensin C on facilitating E and ED
227 III adsorption was observed by fluorescence microscope (Fig. 4C and Fig. 4D). E proteins
228 and ED III proteins bound more efficiently to the C6/36 cell with *aa* defensin. Additionally,
229 *aa* defensin C showed co-localization with E or ED III protein on the C6/36 (Fig. 4C, merge
230 panel). The same results were observed in membrane stained C6/36 cells. E proteins and ED
231 III proteins bound more efficiently to the C6/36 cell surface with *aa* defensin, and *aa* defensin
232 C also showed co-localization with E or ED III protein on the C6/36 surface (Fig. 4D). Thus
233 indicating that the ED III domain of the JEV E protein responsible for binding with *aa*
234 defensin C.

235

236 **LRP2 is responsible for mosquito defensin mediated JEV adsorption**

237 As an extracellular protein, defensin has been reported to interact with receptors on the
238 cell surface and consequently affect intracellular signaling networks. To define the
239 relationship of defensin/cell surface receptor and adsorption enhancement, we analyzed
240 cell-surface receptors that interact with defensin. We knockdowned the expression of a series of

241 potential receptors on the cell surface through RNA interference (RNAi) and found that
242 lipoprotein receptor-related protein 2 (LRP2) responsible for defensin binding [30, 31]. The
243 results indicated that LRP2 interfered with the interaction between defensin-FITC and C6/36 cells
244 (Fig. 5A and Fig. 5B), thus indicating that LRP2 related to the adsorption of extracellular
245 defensin. We further studied the role of LRP2 on JEV adsorption mediated by defensin. Based on
246 significantly RNA knock down (Fig. S3C), No differences were observed between cells with or
247 without LRP2 interference when infected with JEV alone (Fig. 5C). However, when C6/36 cells
248 were incubated with mixed defensin and JEV, a lower JEV level was observed in LRP2 interfered
249 cells. The JEV mRNA level on LRP2 interference cells was 2.8 fold lower than that of the
250 scramble (Negative control, NC) interference group (Fig. 5C), and both the TCID₅₀ level and
251 fluorescence value decreased significantly (Fig. 5D and Fig. 5E). In *in vivo* mosquito experiments,
252 the mosquitoes were inoculated with LRP2 or NC siRNA for 3 days (Fig. S3D), and inoculated
253 with defensin and JEV mixture. Whole body samples were collected at 3 days after infection. The
254 JEV mRNA level was significantly lower in LRP2-interference group than in the NC group (Fig.
255 5F), thus indicating that LRP2 participated in defensin mediated viral adsorption. Additionally, the
256 results of indirect immunofluorescence were in accordance with the above-mentioned results.

257 Take together, our findings indicated that LRP2 is the cell surface factor responsible for defensin
258 mediated JEV adsorption. LRP2/defensin is a pathway mediates JEV adsorption in mosquito.
259 Lipoprotein receptor-related protein 4 (LRP4) and CXCR4 also showed binding activity with
260 defensin, but this activity did not influence JEV adsorption (Data not shown).

261

262 **Mosquito defensin down-regulates the expression of HSC70B on the C6/36 surface and**
263 **reduces antiviral activity of cell**

264 Defensin can interact with cell-surface receptors and consequently affect signal
265 transduction in cells. Therefore, we employed stable isotope labeling with amino acids in cell
266 culture (SILAC) labeling and mass spectroscopy (MS) methods (Fig. 6A) to determine
267 whether mosquito defensin influences the expression of proteins on cell surface and
268 consequently affects JEV adsorption [32]. Briefly, C6/36 cells were continuously passaged on
269 media with light, medium and heavy stable isotopes. After more than 99.0% cells were
270 labeled with stable isotopes, the cells were then grouped, inoculated with JEV or defensin,
271 and collected according to the plan (Fig. 6A). Cell membrane proteins were extracted for MS
272 analysis. The results showed that HSC70B, a potential mosquito antiviral protein [33], was

273 significantly down-regulated in all defensin, JEV, and defensin + JEV treatments (Fig. 6B).

274 We prepared a rabbit polyclonal antibody against C6/36 HSC70B (UniProt accession number

275 A0A0E3J979) according to the MS results (Fig. S2). Western-blot analysis validated the

276 down-regulation of HSC70B on the C6/36 cell surface in all three treatments (Fig. 6C).

277 Because HSC70B is a potential mosquito antiviral protein, we tested the function of

278 mosquito HSC70B on JEV adsorption and infection. siRNA targeting C6/36 HSC70B was

279 transfected, and the interference efficiency of HSC70B on C6/36 was detected through

280 real-time PCR analysis (Fig. 6D). Afterward, JEV was inoculated to HSC70B interfered

281 C6/36 cells. The JEV adsorption capacity in HSC70B-interference cells was significantly

282 higher than that in NC-interference cells ($p < 0.05$) (Fig. 6E). Additionally, JEV replication

283 level was detected in C6/36 cells treated with HSC70B siRNAs and defensin peptides.

284 Compared to NC group, HSC70B interference significantly heightened the enhancement

285 function of defensin (Fig. 6E). Similarly, we designed siRNA targeting the homologous gene

286 of *cpp* HSC70B. siRNA was injected into *cpp*, and the interference efficiency of HSC70B

287 was detected through real-time PCR (Fig. 6F). JEV mRNA levels were detected at 6 days

288 post infection. Likewise, HSC70B-interfered mosquitoes produced more JEV copies than NC

289 group (Fig. 6G).

290 Two mechanisms underlying the facilitation effect were identified. One was a direct
291 binding effect, enhancing JEV affinity to the cell surface. The other was an indirect effect,
292 weakening the host defense by down-regulating antiviral HSC70B expression.

293

294 **Mosquito defensins facilitate JEV dissemination in salivary gland**

295 To assess the transmission potential of JEV enhanced by mosquito defensins, we
296 detected the virus levels within salivary gland of defensin-treated mosquitoes [34, 35]. Both
297 microinjection and blood meal methods were used in this experiment. JEV and mosquito
298 defensin were mixed before inoculation. Mosquitoes injected with JEV and defensin peptide
299 were collected at 7 or 10 days post infection. Fresh salivary glands were isolated and detected
300 by using real time PCR. JEV level were significantly increased in *Cpp* and *aa* defensin groups
301 (Fig. 7A). JEV level in *Cpp* defensin group indicated 3.5 fold higher at day 7 post infection
302 and 3.1 fold higher at day 10 post infection than that of scramble defensin group in salivary
303 gland. *aa* defensin showed the same role as *Cpp* defensin did. We further employed blood
304 meal to measure the effect of defensin in JEV dissemination in mosquito salivary gland. Five

305 day-old female Mosquitoes were deprived of sucrose and water 24 h prior to blood meal.
306 Mosquitoes were then feed with infectious blood with JEV and defensin peptides for 2 h.
307 Fresh blood was collected from health mice and delivered through Hemotek membrane
308 feeding apparatus. 2ml blood with JEV (5×10^6 TCID₅₀) and peptide (200 μ M) were used for
309 each groups. JEV level in *Cpp* defensin group showed 4.2 fold higher at day 7 and 10 post
310 infection than that of scramble defensin group in salivary gland (Fig. 7B). JEV level in *aa*
311 defensin group also showed higher results than scramble group. These results implied that
312 mosquito defensins facilitate JEV dissemination in mosquitoes and increase transmission
313 potential after infection.

314

315 **Discussion**

316 JEV is a serious mosquito borne disease common in Asia-Pacific tropical and subtropical
317 regions [2, 9, 10]. More than 100,000 people are at risk. Moreover, JEV can cause death or
318 permanent sequelae. Pigs are the reservoir host of the virus. Humans, horses and other
319 animals are dead-end hosts. Mosquitoes, especially *culex*, are the most important vector [4].
320 At present, the prevention and control of JEV mainly relies on vaccine immunization, whose

321 protection time is limited. JEV remains a threat to health and even life for
322 immunocompromised children or older people [6, 7]. With the increasing problem of global
323 warming, the clinical incidence of JEV is increasing [36]. Few mechanistic studies have
324 focused on the JEV transmission by mosquito vectors. It is of practical significance to
325 understand the interaction between JEV and mosquito vectors and the immune escape mode
326 of JEV in controlling this mosquito borne disease.

327 In this study, we analyzed the gene expression of defensin from *Cpp* and *aa*. Defensin A
328 and an unnamed defensin from *Cpp*, defensin A, B and C from *aa* shared high sequence
329 similarity, thus indicating similar functions of these defensins. Subsequently, we confirmed
330 that defensin A and defensin C are the main defensin types of *cpp* and *aa*, respectively. Given
331 the high similarity of the amino acid sequences, we synthesized only *cpp* defensin A and *aa*
332 defensin C in further studies. The nucleotide sequence of *cpp* defensin A (number
333 MH756645) has been submitted to the NCBI database.

334 The up-regulation of defensin after JEV infection was consistent with reports on other
335 flavivirus viruses [37]. The highest up-regulation was observed at 7 days post infection. From
336 the organism perspective, the defensin in the salivary gland and whole body was up-regulated

337 more than that in the midgut. JEV replication in salivary gland, the most sensitive tissue to
338 JEV [18], was positively correlated with defensin level.

339 The mature peptide of defensin was utilized to study the role of mosquito defensin in
340 JEV infection [25, 38]. In general, defensin is fewer than 60 amino acids and is processed
341 from a precursor protein. In this study, mosquito defensin and human defensin β 2 were
342 composed of 40 amino acids and 34 amino acids [39], respectively. Only 11% sequence
343 similarity was identified between mosquito and human defensin. Unexpectedly, mosquito
344 defensin facilitated JEV infection, in contrast to human defensin, but the facilitation effect
345 was exerted only on mosquito cells or mosquitoes. Thus, JEV utilized the host defense
346 system, reflecting its “intelligence” in infection [40]. However, mosquito defensin inhibited
347 JEV infection in mammalian cells, thus indicating its varied mechanisms of action and the
348 complicated interaction between virus and host [19].

349 Further analysis demonstrated that mosquito defensin facilitated JEV adsorption to target
350 cells by directly binding JEV virions [27, 41]. By screening JEV structural proteins, we found
351 that mosquito defensin bound the ED III domain of JEV E. ED III is a crucial domain of JEV
352 that is responsible for the production of neutralizing antibody [42]. The antiviral effect of

353 mosquito defensin on JEV is likely to be due to its binding the ED III domain and subsequent
354 virion destruction [19, 25]. Because mosquito defensin facilitated JEV infection, the binding
355 of defensin and ED III can be inferred to have only weak antiviral effects. Nevertheless, this
356 binding enhanced virion adsorption ability to a large extent. The broad transmission of JEV
357 by mosquitoes is ascribed to both the crude immune system of mosquitoes and the infection
358 strategy of the virus. Mosquito defensin could improve the adsorption ability of JEV on target
359 cells. Additionally, ELISA results showed that high concentration of mosquito defensin
360 interacted with the target cells without the assistance of viruses.

361 Defensin receptors expressed on the cell surface may lead to enhanced adsorption. We
362 scanned the potential cell-surface receptor proteins of defensin through RNAi and found that
363 the LRP2-defensin pathway was responsible for JEV adsorption. In mammalian animals,
364 LRP2 is the receptor for defensin, regulating the contraction of smooth muscle cells by
365 combining with human alpha defensin [30, 31]. However, the roles of LRP2 in mosquitoes
366 have not been reported. In the present study, we demonstrated that LRP2 participates in JEV
367 adsorption mediated by defensin. JEV first binds defensin, and then, owing to the affinity of
368 defensin for LRP2, the defensin/JEV complex adsorbs to the cell surface more readily,

369 thereby increasing the chance of infection. This proposed mechanism of promotion of JEV
370 infection by defensin/LRP2 is similar to that for JEV and WNV mediated by C type
371 lectin/PTP-1. That is, virus first combines with extracellular secrete proteins with high
372 affinity to cells, and this is followed by binding to cell surface receptor to infect target cells.

373 Given that mosquito defensin directly interacts with mosquito cell surface receptors, we
374 analyzed how it regulates cell surface proteins. The changes in cell surface proteins were
375 determined through SILAC and MS analysis [32]. We identified a potential antiviral protein,
376 HSC70B, that is significantly down-regulated by defensin or JEV treatment [33]. HSC70B
377 inhibited JEV adsorption, as demonstrated through an RNAi approach, thus indicating that
378 mosquito defensin indirectly affects JEV adsorption by regulating cell surface antiviral
379 protein expression. However, this indirect effect was found to be lower than the direct
380 defensin binding effect. Together, our findings indicated that the effect of mosquito defensin
381 on JEV is composed of weak antiviral effect, direct binding enhancement and indirect
382 immune regulation. Curiously, both defensin and HSC70B are antiviral proteins in mosquito,
383 but it looks like they could't work together on JEV infection. We did not identify the
384 mechanisms through which defensin down-regulates HSC70B, because of the limited

385 information available on the relevant signal pathways. We deduced that there is a negative
386 feedback mechanism between HSC70B and defensin [43], thus implying that an increase in
387 defensin would decrease HSC70B level. Another possibility may be that HSC70B has
388 varying functions in different conditions, except for the antiviral effect.

389 JEV infection up-regulated mosquito defensin expression in the salivary gland and
390 defensin also heightened the JEV dissemination in salivary gland, thus suggesting that the
391 defensin may be influence the transmission of JEV by mosquito. Further research on
392 mosquito defensin in JEV cross-species transmission is needed.

393 To our knowledge, this is the first report on the effects of mosquito defensin on JEV
394 infection in mosquito vectors, revealing a new immune escape mechanism of JEV infection
395 and transmission. This study broadens our knowledge of transmission of JEV as well as other
396 mosquito borne viruses, providing novel insights into viral transmission mechanisms.

397

398 **Materials and methods**

399 **Ethics statement**

400 All animal experiments were performed in compliance with the Guidelines on the

401 Humane Treatment of Laboratory Animals (Ministry of Science and Technology of the
402 People's Republic of China, Policy No. 2006 398) and were approved by the Institutional
403 Animal Care and Use Committee at the Shanghai Veterinary Research Institute (IACUC No:
404 Shvri-Pi-0124).

405

406 **Cells, defensin and viruses**

407 Baby hamster kidney (BHK-21) and African green monkey kidney (Vero) cells were
408 purchased from the ATCC (Rockville, Maryland) and maintained in Dulbecco's modified
409 Eagle's medium (DMEM) supplemented with 10% FBS at 37°C in a 5% CO₂ incubator.
410 C6/36 cells (ATCC) were cultured in RPMI-1640 medium supplemented with 10% FBS at
411 28°C.

412 Mature *Cpp* defensin A (NCBI accession number: MH756645), *aa* defensin C (NCBI
413 accession number: XP_019527114.1), human defensin β 2 (NCBI accession number:
414 NP_004933.1) and scrambled defensin peptides (purity \geq 99%) were synthesized by
415 WC-Gene Biotech Ltd. (Shanghai, China). The amino acid sequences are shown in [Table S3](#).
416 The defensins were dissolved in DMSO (for cell, *ex vivo* or *in vivo* experiments) or PBS (for
417 ELISA detection) and stored at room temperature. Defensins labeled with FITC were kept in

418 the dark at room temperature.

419 JEV strain N28 (NCBI accession number: GU253951.1) was stored in our laboratory and
420 propagated in C6/36 cells. The TCID₅₀ and MID₅₀ of the virus were measured in BHK-21
421 cells or female mosquitoes and calculated by the Reed-Muench method [17, 44].

422

423 **Infection and RNA interference *in vitro***

424 Defensins or scrambled defensin peptides were pre-mixed with JEV (MOI=0.1) at 4°C,
425 then inoculated into cells. C6/36 cells were incubated at 28°C for 2 h. Vero and BHK-21 cells
426 were incubated at 37°C for 2 h. At 24–120 h post infection, the supernatant or cells were
427 collected. Viral titer was determined by TCID₅₀ method and mRNA expression levels were
428 measured by real-time PCR. To determine JEV adsorption, defensins were pre-mixed with
429 JEV at 4°C for 2 h. C6/36 cells were incubated with the mixture on ice for different times.
430 Unabsorbed JEV was removed by washing with PBS for three times. The cells were collected
431 for JEV E mRNA quantification or other measurements.

432 For the *in vitro* RNA interference, siRNA (Table S1) was transfected into C6/36 cells
433 with Cellfectin II reagent (Invitrogen). JEV was inoculated at 24 h post transfection. At 72 h

434 post infection, the cells were collected. Total RNA was isolated, and the viral or gene load
435 was determined by real-time PCR.

436

437 **Infection and RNA interference *in vivo***

438 For *in vivo* experiments, 10-fold serial dilutions were made from a $10^{9.3}$ TCID₅₀ JEV
439 stock. Cold-anesthetized 5 day old female mosquitoes were randomly divided into various
440 groups ($n \geq 13$). Both microinjection and blood meal methods were carried out in infection
441 experiment. For microinjection, the mosquitoes were infected by microinjection (250 nL) into
442 the thorax. An Eppendorf CellTram oil microinjector and 15 μ m needles were used for
443 injecting the mosquitoes. Control mosquitoes were injected with an equivalent volume of
444 PBS [17, 18, 45]. The mosquitoes were harvested, and the viral loading was quantified. For
445 blood meal, fresh blood of specific pathogen free mouse was collected in tubes with
446 anticoagulant. Virus or defensin peptides were mixed and added into fresh blood before
447 feeding. 2 ml blood was used in blood meal by Hemotek FU1 Feeder for each group [34, 46].

448 *In vivo* RNAi was performed as described previously [18]. The siRNA targeting the *Cpp*
449 genes was synthesized by Genepharma (Shanghai, China). The sequences are shown in [Table](#)

450 **S1.** For RNAi and virus challenge, female mosquitoes at 5 days after eclosion were injected
451 into the thorax with 2 μ g dsRNA in 250 nL PBS. After a 3 day recovery period, the
452 mosquitoes were microinjected with JEV at different MID₅₀ in 250 nL PBS for functional
453 studies.

454

455 **RNA isolation and real-time PCR**

456 For real-time PCR, RNA was extracted from cell suspensions or mosquito samples by
457 Qiagen total RNA isolation kit according to the manufacturer's instructions. The RNA
458 concentration was measured by NanoDrop spectrophotometer. cDNA was generated by RT
459 Master reverse transcription kit (Takara) according to the manufacturer's instructions.
460 Real-time quantitative PCR experiments were performed in ABI Prism 7500
461 sequence-detection system (Applied Biosystems, Foster City, CA) with SYBR Green PCR
462 Master Mix (Takara) according to the manufacturer's instructions. The primer sequences are
463 listed in Table 1. The thermal cycling conditions were as follows: 10 min at 95°C, followed
464 by 40 cycles of 95°C for 5 s and 60°C for 1 min. All experiments were performed in
465 triplicate, and gene expression levels are presented relative to those of β -actin. The fold

466 change in relative gene expression compared with the control was determined with the
467 standard $2^{-\Delta\Delta C_t}$ method.

468

469 **Virus titer**

470 Supernatants were harvested from cell cultures for TCID₅₀ assays as described
471 previously [18]. Briefly, BHK-21 cells were seeded on a 96-well plate and grown to 60%
472 confluence. The supernatants were diluted in a 10-fold dilution series and added to each well
473 of the 96-well plate. One hundred microliters of each dilution was added in eight replicate
474 wells, and eight replicate mock controls were set. The plates were incubated at 37°C for 1.5 h.
475 Then the supernatants were discarded and replaced with 100 µL of DMEM supplemented
476 with 1% FBS. After 5 days in culture, the cytopathic effect was recorded. The TCID₅₀ of the
477 virus was calculated by Reed-Muench method [44].

478

479 **Indirect immunofluorescence and western blotting**

480 Indirect immunofluorescence and western blotting were performed as described
481 previously [18]. The antibodies used were mouse anti JEV E monoclonal antibody, rabbit anti

482 mosquito β actin polyclonal antibody, rabbit anti mosquito HSC70B polyclonal antibody,
483 goat anti-mouse IgG-HRP antibody (1:10000; Santa Cruz), Alexa Fluor 405-conjugated
484 anti-mouse IgG antibody (1:500; Abcam), Alexa Fluor 488-conjugated anti-rabbit IgG
485 antibody (1:500; Thermo Fisher Scientific) and Alexa Fluor 594-conjugated anti-rabbit IgG
486 antibody (1:500; Thermo Fisher Scientific). DAPI and Did were used for nucleus and
487 membrane staining. Immunofluorescence was imaged with a Nikon C1Si confocal laser
488 scanning microscope.

489 For tissue immunofluorescence assays, salivary glands were isolated on sialylated slides,
490 washed with PBS, fixed with 4% paraformaldehyde for 1 h, and blocked in PBS with 2%
491 bovine serum albumin (BSA) at room temperature for 2 h. The samples were incubated with
492 mixture of JEV and *cpp* defensin A-FITC, detected with mouse anti JEV E monoclonal
493 antibody and imaged with a Nikon C1Si confocal laser scanning microscope.

494

495 **Protein expression and ELISA**

496 The purified JEV structural proteins (C, M, E, ED III) from the S2 insect expression
497 system (Invitrogen) were quantified by using the bicinchoninic acid (BCA) assay. Expressed

498 proteins were used for ELISA or IFA analysis [47].

499 For defensin ELISA, defensin peptide was dissolved in PBS, then was diluted with 0.1
500 M dicarbonate (pH 9.6) to a final concentration of 250–750 ng. The plate was coated
501 overnight and incubated with 2% BSA for 2 h. Afterward, 100 μ L JEV virus (1×10^5 TCID₅₀)
502 was added and incubated for 30 min at room temperature. The wells were washed with PBST
503 five times, mouse polyclonal antibody to JEV was added to the wells and incubated for 30
504 min. The wells were washed with PBST five times, and goat anti-mouse antibody labeled
505 with HRP was added. After incubation at room temperature 30 min and washing with PBST
506 five times, TMB was added to the wells as a chromogenic substrate. The plate was developed
507 in the dark for 10 min, and H₂SO₄ was added to stop the reaction. The absorbance of each
508 well was read at 450 nm.

509 For viral protein ELISA, purified JEV structural proteins diluted in 0.1 M dicarbonate
510 (pH 9.6) were added to the plate wells. The plate was coated overnight and incubated with 2%
511 BSA for 2 h. Then 100 μ L defensin (50 μ M) labeled with FITC was added. The plate was
512 incubated for 30 min at room temperature and washed with PBST five times before
513 fluorescence measurement.

514 For C6/36 cell ELISA, the plates were pre-treated with polylysine. Healthy and fresh
515 C6/36 cells were counted and diluted with 0.1 M dicarbonate (pH 9.6) to a final concentration
516 of 1×10^5 cells per well. The plate was processed as described above for JEV structural
517 proteins or defensin coated ELISA.

518

519 **SILAC/MS analysis**

520 C6/36 cells were continuously passaged for eight generations on media with light,
521 medium and heavy isotopes. All three labeling efficiencies reached 99%. The cells were
522 grouped, inoculated with JEV or defensin, and collected at 24 h or 48 h according to the
523 procedure. Equal amounts of cells from light, medium and heavy media in the same group
524 were mixed to extract cell membrane proteins according to the manufacturer's instructions
525 (Pierce). Extracted membrane proteins were quantified by BCA, identified by MS and
526 normalized for further analysis.

527

528 **Statistical analysis**

529 All experiments were carried out in at least triplicate. Mean values \pm standard deviation

530 (SD) were calculated in Microsoft Excel. Statistical analysis was done with Student's t tests,
531 and values were considered significant when $p < 0.05$. Figures were created in GraphPad™
532 Prism 5.0 software.

533

534 **Competing interests**

535 The authors declare no competing interests.

536

537 **Acknowledgments**

538 This work was supported by the the National Key Research and Development Program
539 of China (No. 2017YFD0501805, 2018YFD0500101), the Shanghai Natural Science
540 foundation (no. 18ZR1448900), applied research on disease prevention and controls in
541 military (No. 13BJYZ27), the National S & T Major Program (No. 2012ZX10004-220).

542

543 **Reference**

- 544 1. Daep CA, Munoz-Jordan JL, Eugenin EA. Flaviviruses, an expanding threat in public health:
545 focus on dengue, West Nile, and Japanese encephalitis virus. J Neurovirol. 2014;20(6):539-60. doi:
546 10.1007/s13365-014-0285-z. PubMed PMID: 25287260; PubMed Central PMCID: PMC4331079.
- 547 2. Le Flohic G, Porphyre V, Barbazan P, Gonzalez JP. Review of climate, landscape, and viral
548 genetics as drivers of the Japanese encephalitis virus ecology. PLoS Negl Trop Dis. 2013;7(9):e2208.

- 549 doi: 10.1371/journal.pntd.0002208. PubMed PMID: 24069463; PubMed Central PMCID:
550 PMC3772072.
- 551 3. Zheng Y, Li M, Wang H, Liang G. Japanese encephalitis and Japanese encephalitis virus in
552 mainland China. *Rev Med Virol.* 2012;22(5):301-22. doi: 10.1002/rmv.1710. PubMed PMID:
553 22407526.
- 554 4. Huang YJ, Higgs S, Horne KM, Vanlandingham DL. Flavivirus-mosquito interactions. *Viruses.*
555 2014;6(11):4703-30. doi: 10.3390/v6114703. PubMed PMID: 25421894; PubMed Central PMCID:
556 PMC4246245.
- 557 5. Mansfield KL, Hernandez-Triana LM, Banyard AC, Fooks AR, Johnson N. Japanese encephalitis
558 virus infection, diagnosis and control in domestic animals. *Vet Microbiol.* 2017;201:85-92. doi:
559 10.1016/j.vetmic.2017.01.014. PubMed PMID: 28284628.
- 560 6. Yun SI, Lee YM. Japanese encephalitis: the virus and vaccines. *Hum Vaccin Immunother.*
561 2014;10(2):263-79. doi: 10.4161/hv.26902. PubMed PMID: 24161909; PubMed Central PMCID:
562 PMC4185882.
- 563 7. Barzon L, Palu G. Recent developments in vaccines and biological therapies against Japanese
564 encephalitis virus. *Expert Opin Biol Ther.* 2018;18(8):851-64. doi: 10.1080/14712598.2018.1499721.
565 PubMed PMID: 29991325.
- 566 8. Chokephaibulkit K, Houillon G, Feroldi E, Bouckenoghe A. Safety and immunogenicity of a
567 live attenuated Japanese encephalitis chimeric virus vaccine (IMOJEV(R)) in children. *Expert Rev*
568 *Vaccines.* 2016;15(2):153-66. doi: 10.1586/14760584.2016.1123097. PubMed PMID: 26588242.
- 569 9. Heffelfinger JD, Li X, Batmunkh N, Grabovac V, Diorditsa S, Liyanage JB, et al. Japanese
570 Encephalitis Surveillance and Immunization - Asia and Western Pacific Regions, 2016. *MMWR Morb*
571 *Mortal Wkly Rep.* 2017;66(22):579-83. doi: 10.15585/mmwr.mm6622a3. PubMed PMID: 28594790;
572 PubMed Central PMCID: PMC5720240.
- 573 10. Centers for Disease C, Prevention. Japanese encephalitis surveillance and immunization--Asia
574 and the Western Pacific, 2012. *MMWR Morb Mortal Wkly Rep.* 2013;62(33):658-62. PubMed PMID:
575 23965828; PubMed Central PMCID: PMC4604796.
- 576 11. Huang YS, Hettenbach SM, Park SL, Higgs S, Barrett AD, Hsu WW, et al. Differential
577 Infectivities among Different Japanese Encephalitis Virus Genotypes in *Culex quinquefasciatus*
578 Mosquitoes. *PLoS Negl Trop Dis.* 2016;10(10):e0005038. doi: 10.1371/journal.pntd.0005038. PubMed
579 PMID: 27706157; PubMed Central PMCID: PMC5051684.
- 580 12. Conway MJ, Colpitts TM, Fikrig E. Role of the Vector in Arbovirus Transmission. *Annu Rev*
581 *Virol.* 2014;1(1):71-88. doi: 10.1146/annurev-virology-031413-085513. PubMed PMID: 26958715.

- 582 13. Takahashi M, Suzuki K. Japanese encephalitis virus in mosquito salivary glands. *Am J Trop Med*
583 *Hyg.* 1979;28(1):122-35. PubMed PMID: 219722.
- 584 14. Ahlers LRH, Goodman AG. The Immune Responses of the Animal Hosts of West Nile Virus: A
585 Comparison of Insects, Birds, and Mammals. *Front Cell Infect Mi.* 2018;8. doi: Artn 96
586 10.3389/Fcimb.2018.00096. PubMed PMID: WOS:000429048200001.
- 587 15. Pakpour N, Riehle MA, Luckhart S. Effects of ingested vertebrate-derived factors on insect
588 immune responses. *Curr Opin Insect Sci.* 2014;3:1-5. doi: 10.1016/j.cois.2014.07.001. PubMed PMID:
589 WOS:000209578700002.
- 590 16. Strand MR. The insect cellular immune response. *Insect Sci.* 2008;15(1):1-14. doi:
591 10.1111/j.1744-7917.2008.00183.x. PubMed PMID: WOS:000252587700001.
- 592 17. Cheng G, Cox J, Wang P, Krishnan MN, Dai J, Qian F, et al. A C-type lectin collaborates with a
593 CD45 phosphatase homolog to facilitate West Nile virus infection of mosquitoes. *Cell.*
594 2010;142(5):714-25. doi: 10.1016/j.cell.2010.07.038. PubMed PMID: 20797779; PubMed Central
595 PMCID: PMC2954371.
- 596 18. Liu K, Qian Y, Jung YS, Zhou B, Cao R, Shen T, et al. mosGCTL-7, a C-Type Lectin Protein,
597 Mediates Japanese Encephalitis Virus Infection in Mosquitoes. *J Virol.* 2017;91(10). doi:
598 10.1128/JVI.01348-16. PubMed PMID: 28250133; PubMed Central PMCID: PMC5411588.
- 599 19. Klotman ME, Chang TL. Defensins in innate antiviral immunity. *Nat Rev Immunol.*
600 2006;6(6):447-56. doi: 10.1038/nri1860. PubMed PMID: 16724099.
- 601 20. Schmid-Hempel P. Evolutionary ecology of insect immune defenses. *Annu Rev Entomol.*
602 2005;50:529-51. doi: 10.1146/annurev.ento.50.071803.130420. PubMed PMID: 15471530.
- 603 21. Yasin B, Wang W, Pang M, Cheshenko N, Hong T, Waring AJ, et al. Theta defensins protect
604 cells from infection by herpes simplex virus by inhibiting viral adhesion and entry. *J Virol.*
605 2004;78(10):5147-56. PubMed PMID: 15113897; PubMed Central PMCID: PMC400355.
- 606 22. Wang W, Owen SM, Rudolph DL, Cole AM, Hong T, Waring AJ, et al. Activity of alpha- and
607 theta-defensins against primary isolates of HIV-1. *J Immunol.* 2004;173(1):515-20. PubMed PMID:
608 15210812.
- 609 23. Munk C, Wei G, Yang OO, Waring AJ, Wang W, Hong T, et al. The theta-defensin, retrocyclin,
610 inhibits HIV-1 entry. *AIDS Res Hum Retroviruses.* 2003;19(10):875-81. doi:
611 10.1089/088922203322493049. PubMed PMID: 14585219.
- 612 24. Meyerholz DK, Grubor B, Gallup JM, Lehmkuhl HD, Anderson RD, Lazic T, et al.
613 Adenovirus-mediated gene therapy enhances parainfluenza virus 3 infection in neonatal lambs. *J Clin*
614 *Microbiol.* 2004;42(10):4780-7. doi: 10.1128/JCM.42.10.4780-4787.2004. PubMed PMID: 15472341;

- 615 PubMed Central PMCID: PMC522350.
- 616 25. Wilson SS, Wiens ME, Smith JG. Antiviral Mechanisms of Human Defensins. *J Mol Biol.*
617 2013;425(24):4965-80. doi: 10.1016/j.jmb.2013.09.038. PubMed PMID: WOS:000328808500008.
- 618 26. Kota S, Sabbah A, Chang TH, Harnack R, Xiang Y, Meng X, et al. Role of human
619 beta-defensin-2 during tumor necrosis factor-alpha/NF-kappaB-mediated innate antiviral response
620 against human respiratory syncytial virus. *J Biol Chem.* 2008;283(33):22417-29. doi:
621 10.1074/jbc.M710415200. PubMed PMID: 18567888; PubMed Central PMCID: PMC2504899.
- 622 27. Cox RG, Mainou BA, Johnson M, Hastings AK, Schuster JE, Dermody TS, et al. Human
623 Metapneumovirus Is Capable of Entering Cells by Fusion with Endosomal Membranes. *PLoS Path.*
624 2015;11(12). doi: ARTN e1005303
625 10.1371/journal.ppat.1005303. PubMed PMID: WOS:000368332800025.
- 626 28. Kallio J, Leinonen A, Ulvila J, Valanne S, Ezekowitz RA, Ramet M. Functional analysis of
627 immune response genes in *Drosophila* identifies JNK pathway as a regulator of antimicrobial peptide
628 gene expression in S2 cells. *Microbes Infect.* 2005;7(5-6):811-9. doi: 10.1016/j.micinf.2005.03.014.
629 PubMed PMID: 15890554.
- 630 29. Luca VC, AbiMansour J, Nelson CA, Fremont DH. Crystal Structure of the Japanese Encephalitis
631 Virus Envelope Protein. *J Virol.* 2012;86(4):2337-46. doi: 10.1128/Jvi.06072-11. PubMed PMID:
632 WOS:000299862500041.
- 633 30. Higazi AA, Nassar T, Ganz T, Rader DJ, Udassin R, Bdeir K, et al. The alpha-defensins stimulate
634 proteoglycan-dependent catabolism of low-density lipoprotein by vascular cells: a new class of
635 inflammatory apolipoprotein and a possible contributor to atherogenesis. *Blood.* 2000;96(4):1393-8.
636 PubMed PMID: WOS:000089578200027.
- 637 31. Nassar T, Akkawi S, Bar-Shavit R, Haj-Yehia A, Bdeir K, Al-Mehdi AB, et al. Human
638 alpha-defensin regulates smooth muscle cell contraction: a role for low-density lipoprotein
639 receptor-related protein/alpha 2-macroglobulin receptor. *Blood.* 2002;100(12):4026-32. doi: DOI
640 10.1182/blood-2002-04-1080. PubMed PMID: WOS:000179453700023.
- 641 32. Emmott E, Wise H, Loucaides EM, Matthews DA, Digard P, Hiscox JA. Quantitative proteomics
642 using SILAC coupled to LC-MS/MS reveals changes in the nucleolar proteome in influenza A
643 virus-infected cells. *J Proteome Res.* 2010;9(10):5335-45. doi: 10.1021/pr100593g. PubMed PMID:
644 20701360.
- 645 33. Sim C, Hong YS, Tsetsarkin KA, Vanlandingham DL, Higgs S, Collins FH. *Anopheles gambiae*
646 heat shock protein cognate 70B impedes o'nyong-nyong virus replication. *BMC Genomics.*
647 2007;8:231. doi: 10.1186/1471-2164-8-231. PubMed PMID: 17625007; PubMed Central PMCID:

- 648 PMC1963456.
- 649 34. Armstrong PM, Ehrlich HY, Magalhaes T, Miller MR, Conway PJ, Bransfield A, et al.
650 Successive blood meals enhance virus dissemination within mosquitoes and increase transmission
651 potential. #N/A. 2020;5(2):239-+. doi: 10.1038/s41564-019-0619-y. PubMed PMID:
652 WOS:000511211600007.
- 653 35. Kilpatrick AM, Meola MA, Moudy RM, Kramer LD. Temperature, viral genetics, and the
654 transmission of West Nile virus by *Culex pipiens* mosquitoes. *PLoS Path.* 2008;4(6). doi: ARTN
655 e1000092
656 10.1371/journal.ppat.1000092. PubMed PMID: WOS:000259782800014.
- 657 36. Reeves WC, Hardy JL, Reisen WK, Milby MM. Potential effect of global warming on
658 mosquito-borne arboviruses. *J Med Entomol.* 1994;31(3):323-32. PubMed PMID: 8057305.
- 659 37. Xiao X, Liu Y, Zhang X, Wang J, Li Z, Pang X, et al. Complement-related proteins control the
660 flavivirus infection of *Aedes aegypti* by inducing antimicrobial peptides. *PLoS Path.*
661 2014;10(4):e1004027. doi: 10.1371/journal.ppat.1004027. PubMed PMID: 24722701; PubMed Central
662 PMCID: PMC3983052.
- 663 38. Harwig SS, Park AS, Lehrer RI. Characterization of defensin precursors in mature human
664 neutrophils. *Blood.* 1992;79(6):1532-7. PubMed PMID: 1547345.
- 665 39. Mansour SC, Pena OM, Hancock REW. Host defense peptides: front-line immunomodulators.
666 *Trends Immunol.* 2014;35(9):443-50. doi: 10.1016/j.it.2014.07.004. PubMed PMID:
667 WOS:000342269900007.
- 668 40. Gack MU, Diamond MS. Innate immune escape by Dengue and West Nile viruses. *Curr Opin*
669 *Virol.* 2016;20:119-28. doi: 10.1016/j.coviro.2016.09.013. PubMed PMID: 27792906; PubMed Central
670 PMCID: PMC5578430.
- 671 41. Mercer J, Schelhaas M, Helenius A. Virus entry by endocytosis. *Annu Rev Biochem.*
672 2010;79:803-33. doi: 10.1146/annurev-biochem-060208-104626. PubMed PMID: 20196649.
- 673 42. Lin CW, Wu SC. A functional epitope determinant on domain III of the Japanese encephalitis
674 virus envelope protein interacted with neutralizing-antibody combining sites. *J Virol.*
675 2003;77(4):2600-6. PubMed PMID: 12551998; PubMed Central PMCID: PMC141121.
- 676 43. Kim MJ, Hwang SY, Imaizumi T, Yoo JY. Negative feedback regulation of RIG-I-mediated
677 antiviral signaling by interferon-induced ISG15 conjugation. *J Virol.* 2008;82(3):1474-83. doi:
678 10.1128/JVI.01650-07. PubMed PMID: 18057259; PubMed Central PMCID: PMC2224411.
- 679 44. Pizzi M. Sampling variation of the fifty percent end-point, determined by the Reed-Muench
680 (Behrens) method. *Hum Biol.* 1950;22(3):151-90. PubMed PMID: 14778593.

- 681 45. Blandin S, Moita LF, Kocher T, Wilm M, Kafatos FC, Levashina EA. Reverse genetics in the
682 mosquito *Anopheles gambiae*: targeted disruption of the Defensin gene. *EMBO Rep.* 2002;3(9):852-6.
683 doi: 10.1093/embo-reports/kvf180. PubMed PMID: 12189180; PubMed Central PMCID:
684 PMC1084233.
- 685 46. Zhu YB, Tong LQ, Nie KX, Wiwatanaratanaabutr I, Sun P, Li QQ, et al. Host serum iron
686 modulates dengue virus acquisition by mosquitoes. *Nat Microbiol.* 2019;4(12):2405-15. doi:
687 10.1038/s41564-019-0555-x. PubMed PMID: WOS:000499071100041.
- 688 47. Muerhoff AS, Dawson GJ, Dille B, Gutierrez R, Leary TP, Gupta MC, et al. Enzyme-linked
689 immunosorbent assays using recombinant envelope protein expressed in COS-1 and *Drosophila* S2
690 cells for detection of West Nile virus immunoglobulin M in serum or cerebrospinal fluid. *Clin Diagn*
691 *Lab Immunol.* 2004;11(4):651-7. doi: 10.1128/CDLI.11.4.651-657.2004. PubMed PMID: 15242936;
692 PubMed Central PMCID: PMC440607.
- 693

695 **Figure legends**

696 **Fig. 1. JEV infection induced defensin up-regulation in mosquito vectors.**

697 (A) JEV infection curve in mosquitoes. JEV (10^3 MID₅₀) or PBS was inoculated into female
698 mosquitoes by throat injection. Whole body, salivary gland and midgut samples were
699 collected at 4, 7 and 10 days post JEV infection. JEV E expression was quantified by
700 real-time PCR. (B) Expression levels of *cpp* defensins in the whole body. JEV (10^3 MID₅₀) or
701 PBS was inoculated into female mosquitoes by throat injection. *Cpp* defensin A mRNA levels
702 in the whole body at 7 and 10 days post JEV infection were quantified by real-time PCR. (C)
703 Expression levels of *cpp* defensins in the midgut and salivary gland. JEV (10^3 MID₅₀) or PBS
704 was inoculated into female mosquitoes by throat injection. Midgut and salivary gland were
705 separated at 7 days post infection. *Cpp* defensin A mRNA levels were quantified by real-time
706 PCR. (D) One step growth curve of JEV virus in C6/36. C6/36 cells were infected with 5
707 MOI and collected at different time points, as shown in Fig. 1D. JEV E mRNA levels were
708 quantified by real-time PCR. (E) Expression levels of *aa* defensins. C6/36 cells were infected
709 with 5 MOI and collected at 1, 3 and 5 days post JEV infection. *Aa* defensin C and total
710 defensins mRNA levels were quantified by real-time PCR. All experiments were done

711 in triplicate and were performed at least three times. Data are shown as Mean values \pm
712 standard deviations.

713

714 **Fig. 2. Mosquito defensin facilitated JEV infection in mosquito vectors.**

715 (A) Mosquito defensin facilitated JEV infection in *Culex* mosquitoes. Mosquito defensins
716 (100 μ M) and JEV (10 MID₅₀) were pre-mixed at 4°C for 2 h and inoculated into female
717 mosquitoes. JEV E mRNA levels in the whole body at 7 and 10 days post JEV infection were
718 quantified by real-time PCR. (B) Mosquito defensins interference harmed JEV infection in
719 *Culex* mosquitoes. Female mosquitoes were injected with siRNAs for 3 days, then JEV was
720 injected in dose of 10 MID₅₀. JEV E mRNA levels in the whole body at 6 days post JEV
721 infection were quantified by real-time PCR. (C) Mosquito defensins facilitated JEV infection
722 on C6/36 in IFA detection. Mosquito defensins (50 μ M) and JEV (0.5 MOI) were pre-mixed
723 at 4°C and inoculated into C6/36 cells for 2 h (upper three panels). siRNAs target defensin
724 were transfected into C6/36 cell for 24 h, then JEV was inoculated to C6/36 cell for 2 h
725 (lower three panels). IFA was performed on cells at 3 days post infection. Bar, 10 μ m. (D)
726 Mosquito Defensins facilitated JEV infection in C6/36 cells. Mosquito defensins (50 μ M) and

727 JEV (0.5 MOI) were pre-mixed at 4°C and inoculated into C6/36 cells for 2 h. The cells and
728 supernatant were collected at 3 days post infection to quantify JEV E mRNA levels (i) and
729 TCID₅₀ (ii). (E) Defensin knockdown harmed JEV infection in C6/36 cell. siRNAs target
730 defensin were transfected into C6/36 cell for 24 h, then equal JEV was added to C6/36 cell
731 without changing media. The cells and supernatant were collected at 2 days post infection to
732 quantify JEV E mRNA levels (i) and TCID₅₀ (ii). (F - G) Mosquito defensins inhibited JEV
733 infection in mammalian cells. Mosquito defensins (50 µM) and JEV (0.5 MOI) were
734 pre-mixed at 4°C and were inoculated into Vero (F) or BHK (G) for 1.5 h at 37°C. The cells
735 and supernatant were collected at 48 h post infection to quantify JEV E mRNA levels (i) and
736 TCID₅₀ (ii). All experiments were done in triplicate and were performed at least three times.
737 Data are shown as Mean values ± standard deviations.

738

739 **Fig. 3. Mosquito Defensin facilitated JEV adsorption to mosquito cells.**

740 (A) Step scan of JEV infection on C6/36 cell. Steps of JEV infection on C6/36 cell were
741 analyzed by different treatments. For binding, virus (0.5 MOI) and defensin (50 µM) were
742 mixed and inoculated to C6/36 cell on ice for 4 h, washed with PBS for five times, cultured

743 for 48 h with new media. For uncoating, virus (0.5 MOI) was inoculated to C6/36 cell on ice
744 for 4 h, washed with PBS for five times. Fresh media with defensin (50 μ M) was added to cell
745 for 6 h. After incubation, cell was washed and cultured for another 42 h with new media. For
746 replication, virus (0.5 MOI) was inoculated to C6/36 cell on ice for 4 h, washed with PBS for
747 five times. New media without defensin was added to cell for 48 h, and defensin (50 μ M) was
748 added into media at 6 h post culture. The cells were collected to quantify JEV E mRNA levels
749 by real-time PCR. (B) *Aa* defensin C facilitated JEV adsorption to C6/36 in a time-dependent
750 manner. *Aa* defensin C (50 μ M) and JEV (0.5 MOI) were pre-mixed at 4°C and inoculated
751 into C6/36 cells on ice for 4 h. Unabsorbed JEV was removed by washing with PBS three
752 times. The cells were collected to quantify JEV E mRNA levels by real-time PCR. (C and D)
753 IFA assay of JEV adsorption to C6/36 cells. *Aa* defensin C-FITC (50 μ M) and JEV (1 MOI)
754 were pre-mixed at 4°C and inoculated into C6/36 cells on ice. Unabsorbed JEV and defensin
755 were removed by washing with PBS three times. The cells were strained with antibody and
756 DAPI (C) or Did (D). (E) Co-localization of defensin and JEV on the cell surface. *Aa*
757 defensin C-FITC (50 μ M) and JEV (1 MOI) were pre-mixed at 4°C and inoculated into C6/36
758 cells on ice for 2 h, 4 h and 6 h. Unabsorbed JEV and defensin were removed by washing

759 with PBS three times. The cells were treated to observe JEV E (red fluorescence),
760 defensin-FITC (green fluorescence) and nuclei (blue fluorescence). Bar, 10 μ m. (F)
761 Co-localization of *Cpp* defensin A-FITC and JEV on the salivary gland. The salivary glands
762 from uninfected female mosquitoes were freshly isolated. Pre-mixed *cpp* defensin A-FITC
763 (50 μ M) and JEV (1 MOI) were added to salivary glands and incubated at room temperature
764 for 1 h. JEV E was labeled with monoclonal antibody (red fluorescence). Defensin-FITC was
765 detected by green fluorescence, and nuclei were stained with DAPI (blue fluorescence). Bar,
766 20 μ m. (G) JEV bind to defensin. The plate was coated with *aa* defensin C, incubated with
767 JEV and assessed with anti-JEV monoclonal antibody. (H) Defensin and JEV mixture binds
768 to C6/36 cells. The plate after polylysine treatment was coated with C6/36, pre-mixed
769 defensin and JEV were added, and detection was performed with anti-JEV antibody. (I)
770 Defensin binds to C6/36 directly. The polylysine treated plate was coated with C6/36,
771 defensin-FITC were added, and fluorescence value was detected. All experiments were done
772 in triplicate and were performed at least three times. Data are shown as Mean values \pm
773 standard deviations.
774

775 **Fig. 4. Mosquito defensin bound JEV virions.**

776 (A) Viral proteins bind to mosquito defensin. The plate was coated with *aa* defensin C, and
777 incubated with JEV structural proteins. Rabbit polyclonal antibodies to C protein and mouse
778 monoclonal antibody to prM, E and ED III protein were utilized for viral protein binding
779 detection. (B) Mosquito defensin-FITC bind to viral proteins. The plate was coated with
780 purified JEV structural proteins, and incubated with *aa* defensin C-FITC. The fluorescence
781 value of each well was measured. (C and D) Colocalization between defensin and E or ED III
782 proteins. Defensin-FITC and E or ED III were pre-mixed at 4°C and inoculation into C6/36
783 cells on ice for 4 h. Unabsorbed defensin and proteins were removed by washing with PBS
784 three times. (C) The cells were stained with monoclonal antibody and DAPI to observe JEV E
785 (red fluorescence), defensin-FITC (green fluorescence) and nuclei (blue fluorescence). (D)
786 The cells were stained with monoclonal antibody and Did to observe JEV E (cyan
787 fluorescence), defensin-FITC (green fluorescence) and membrane (red fluorescence). Bar, 10
788 µm. All experiments were done in triplicate and were performed at least three times. Data are
789 shown as Mean values ± standard deviations.

790

791 **Fig. 5. LRP2/defensin pathway mediates JEV adsorption.**

792 (A and B) Defensin adsorption was influenced by LRP2. The polylysine treated plate was
793 coated with C6/36, LRP2 siRNAs were transfected into cell. Defensin-FITC was inoculated
794 into cells at 24 h post transfection. After incubation on ice for 2 h, unabsorbed defensin was
795 removed by washing with PBS three times. Fluorescence value was detected by fluorescence
796 analyzer (A) or fluorescence microscope (B). (C, D and E) JEV adsorption on C6/36 cell was
797 influenced by LRP2/defensin pathway. The polylysine treated plate was coated with C6/36,
798 LRP2 siRNAs were transfected into cell. Pre-mixed JEV and *aa* Defensin C was inoculated
799 into cells at 24 h post siRNA transfection. After incubation at room temperature or on ice for
800 2 h, unabsorbed defensin and virus were removed by washing with PBS three times. For
801 real-time PCR (C) and TCID₅₀ (D) measurement, C6/36 cell and supernatant were collected at
802 2 days post infection. For IFA assay, C6/36 cell was treated immediately after inoculation on
803 ice (E). JEV E was labeled with monoclonal antibody (red fluorescence). Defensin-FITC was
804 detected by green fluorescence, and nuclei were stained with DAPI (blue fluorescence). Bar,
805 10 µm. (F) *In vivo* JEV adsorption was influenced by LRP2/defensin pathway. Three days
806 after mosquitoes were injected with LRP2 siRNA, the mosquitoes were injected with

807 pre-mixed JEV and defensin. 6 days post infection, mosquitoes were collected to detect JEV
808 E mRNA levels in whole body. All experiments were done
809 in triplicate and were performed at least three times. Data are shown as Mean values \pm
810 standard deviations.

811

812 **Fig. 6. Defensin down-regulated HSC70B on the C6/36 cell surface to enhance JEV**
813 **adsorption.**

814 (A) SILAC/MS workflow. (B) LC-MS/MS intensity of HSC70B on the C6/36 cell surface.
815 Intensity of HSC70B on cell surface was calculate. Protein levels were normalized in a mass
816 spectrometry computing program. (C) Validation of HSC70B expression on C6/36 cell
817 surface according to SILAC/MS. Mosquito HSC70B was probed by rabbit
818 polyclonal anti-HSC70B antibody. (D) The efficiency of HSC70B RNAi *in vitro*. HSC70B
819 siRNA target *aa* HSC70B was transfected into C6/36 cells for 24 h. Cell was collected and
820 HSC70B mRNA was measured by real-time PCR. (E) HSC70B interference facilitated JEV
821 adsorption to cells. C6/36 cells were inoculated with HSC70B siRNA for 24 h and then
822 inoculated with JEV or JEV and defensin on ice for 4 h. Unabsorbed JEV or defensin was

823 removed by washing with PBS three times. The cells were collected to quantify JEV E
824 mRNA levels by real-time PCR. (F) The efficiencies of RNAi HSC70B *in vivo*. siRNA target
825 *cpp* HSC70B was injected. The mosquitoes were collected at 3 days post injection to detect
826 HSC70B mRNA levels *in vivo*. (G) HSC70B interference facilitated JEV infection *in vivo*.
827 Three days after mosquitoes *in vivo* HSC70B RNAi, the mosquitoes were injected with 10
828 MID₅₀ JEV. Mosquito samples were collected at 6 days post infection, and JEV E mRNA
829 levels were detected by real-time PCR. All experiments were done
830 in triplicate and were performed at least three times. Data are shown as Mean values ±
831 standard deviations.

832

833 **Fig. 7. Mosquito defensin enhanced JEV replication in salivary gland**

834 (A) JEV E mRNA levels within salivary gland based on microinjection. *Cpp* defensin A (100
835 μM) and JEV (10 MID₅₀) were pre-mixed at 4°C for 2 h and injected into female mosquitoes.
836 Salivary glands were isolated at 7 and 10 days post injection and detected by real-time PCR.
837 (B) JEV E mRNA levels within salivary gland based on blood meal. *Cpp* defensin A (100
838 μM) and JEV (10³ MID₅₀) were pre-mixed at 4°C. Mixture was added into fresh blood with

839 anticoagulant. Blood meal was performed for 2 h. Salivary glands were isolated at 7 and 10
840 days post infection and detected by real-time PCR. All experiments were done
841 in triplicate and were performed at least three times. Data are shown as Mean values \pm
842 standard deviations.

843

844 **Supplement Figures**

845 **Fig. S1. Sequence and abundance of mosquito defensins.**

846 (A) Amplification of *cpp* defensin A by PCR. (B) Defensin sequence alignment. Alignment
847 of *cpp* defensin sequences (*Cpp* defensin A and unnamed defensin). (C) Abundance of
848 defensins in C6/36 and *cpp*. Defensin genes were amplified and cloned into pMD18 plasmids,
849 and positive plasmids were used to construct standard curves. Defensin abundance in cells or
850 mosquitoes was quantified with a standard curve through real-time PCR. Defensin abundance
851 is shown as a proportion. Target defensins are shown in gray in columns; the total column
852 represents total defensins. (D, E) Defensin sequence alignment. Alignment of defensins in
853 different mosquito Species (D). Alignment of mosquito defensins and human defensin (E).
854 Alignment was performed by DNAMAN software. Data are shown as Mean values \pm

855 standard deviations.

856

857 **Fig. S2. Major sequences used in this study.**

858 (A) *Culex pipiens pallens* defensin A protein sequence (NCBI number MH756645); the
859 mature defensin sequence is in red. (B) *Culex pipiens pallens* HSC70B partial sequence. (C)
860 *Culex pipiens pallens* unnamed defensin partial sequence. (D) C6/36 HSC70B protein
861 sequence (immunogenic peptide for antibody preparation is in red).

862

863 **Fig. S3. RNA interference efficiency in *in vitro* and *in vivo*.**

864 (A) The efficiency of defensins RNAi *in vivo*. siRNAs target *cpp* total defensins or defensin
865 A were injected. Mosquitoes were collected at 3 days post injection to detect defensins
866 mRNA levels by real-time PCR. (B) The efficiency of defensins RNAi *in vitro*. siRNAs target
867 *aa* defensins was transfected into C6/36 cells for 24 h. Cell was collected and defensins
868 mRNA were measured by real-time PCR. (C) The efficiency of LRP2 RNAi *in vitro*. LRP2
869 siRNA target *aa* LRP2 was transfected into C6/36 cells for 24 h. Cell was collected and LRP2
870 mRNA was measured by real-time PCR. (D) The efficiency of LRP2 RNAi *in vivo*. siRNA

871 target *cpp* LRP2 was injected. Mosquitoes were collected at 3 days post injection to detect
872 LRP2 mRNA levels by real-time PCR. All experiments were done
873 in triplicate and were performed for three times. Data are shown as Mean values \pm standard
874 deviations.

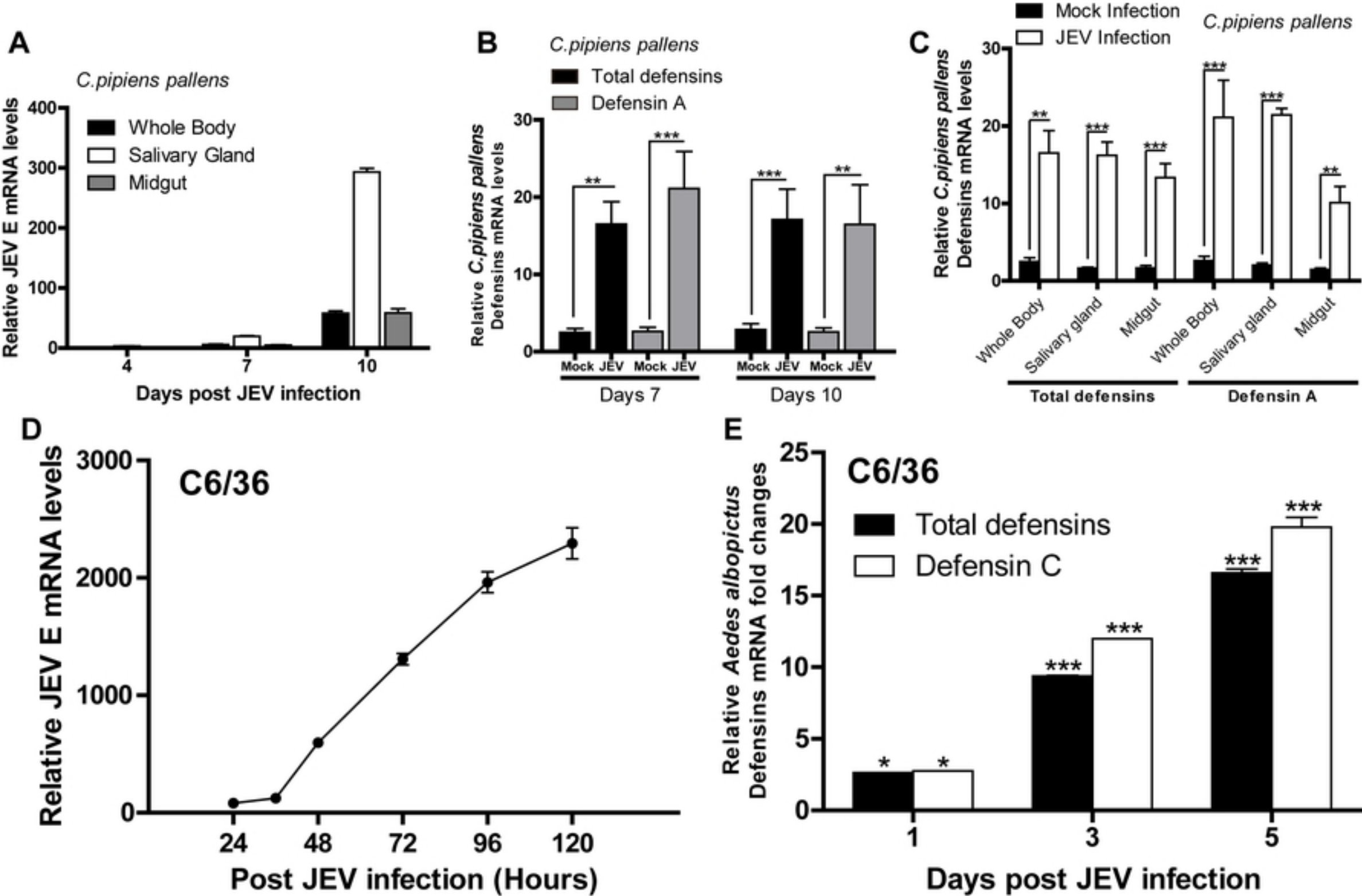


Figure 1

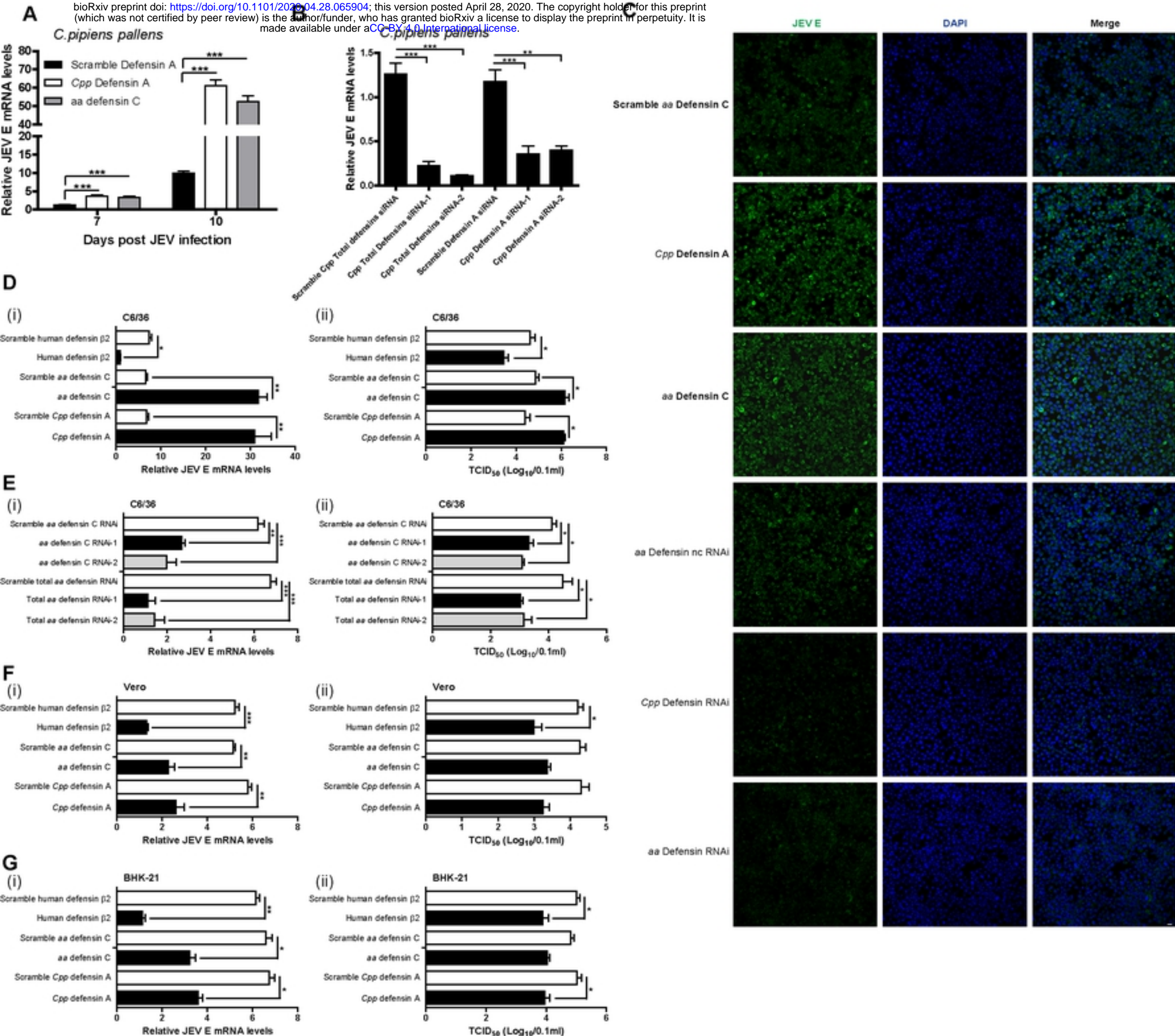


Figure 2

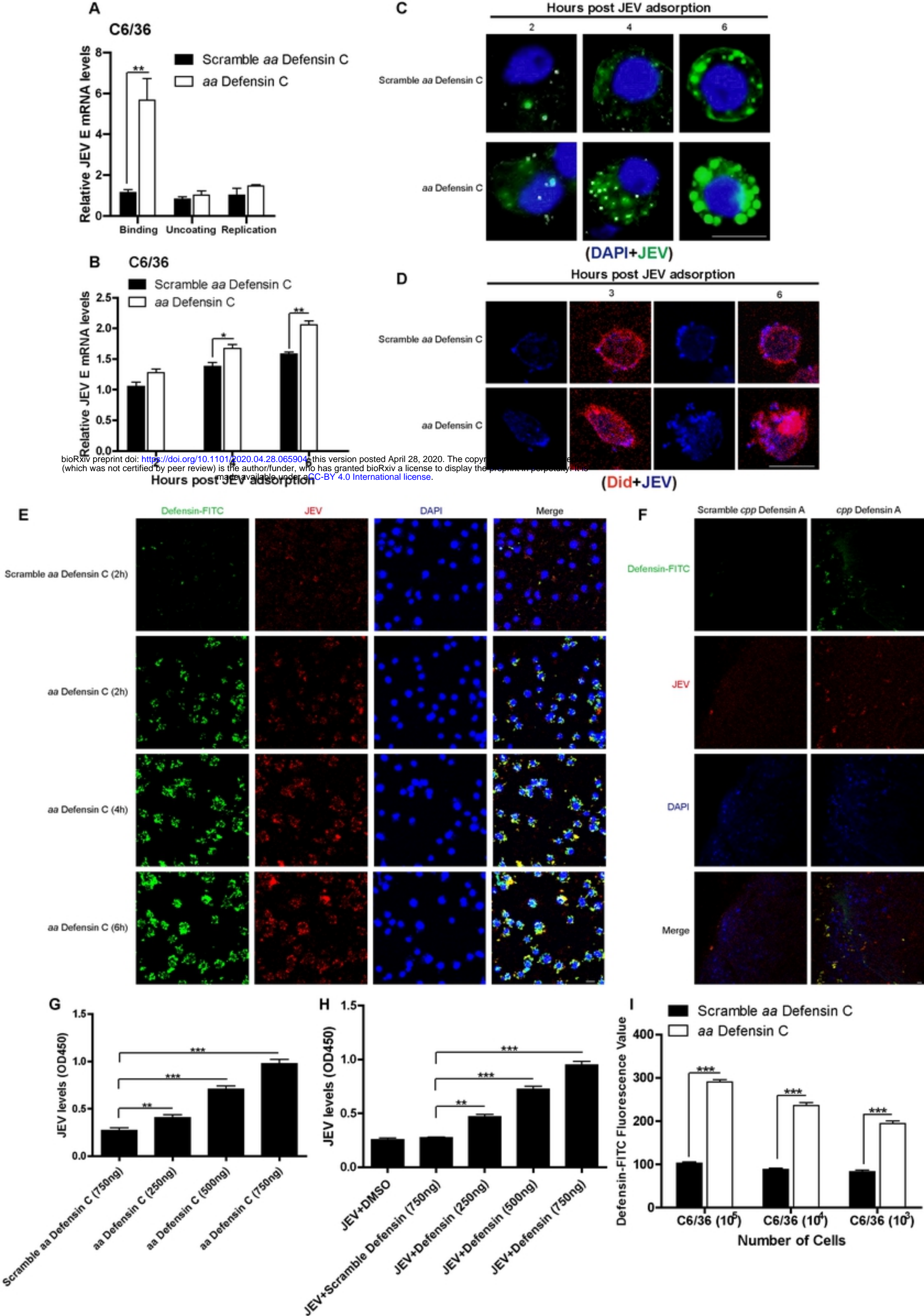


Figure 3

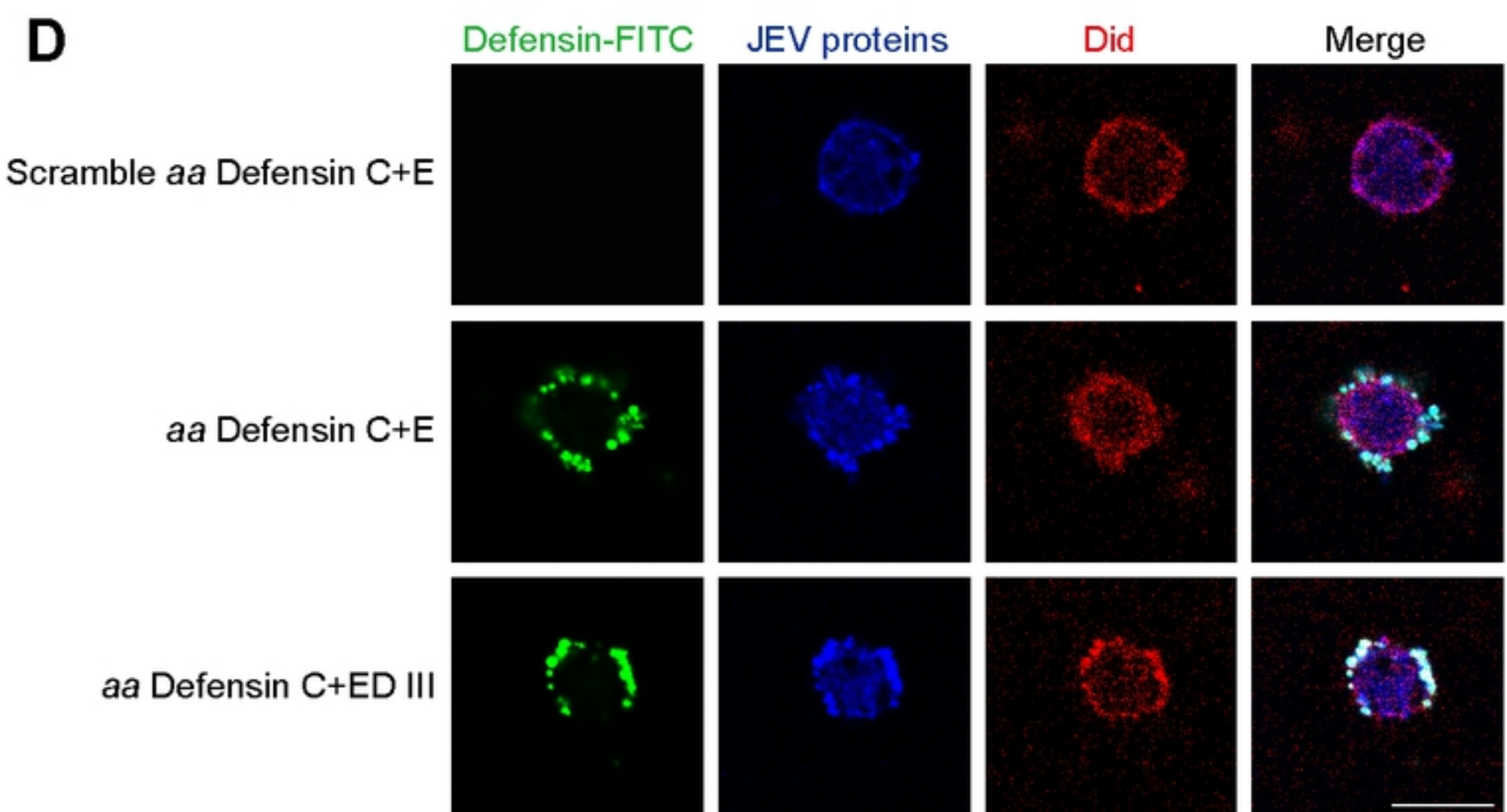
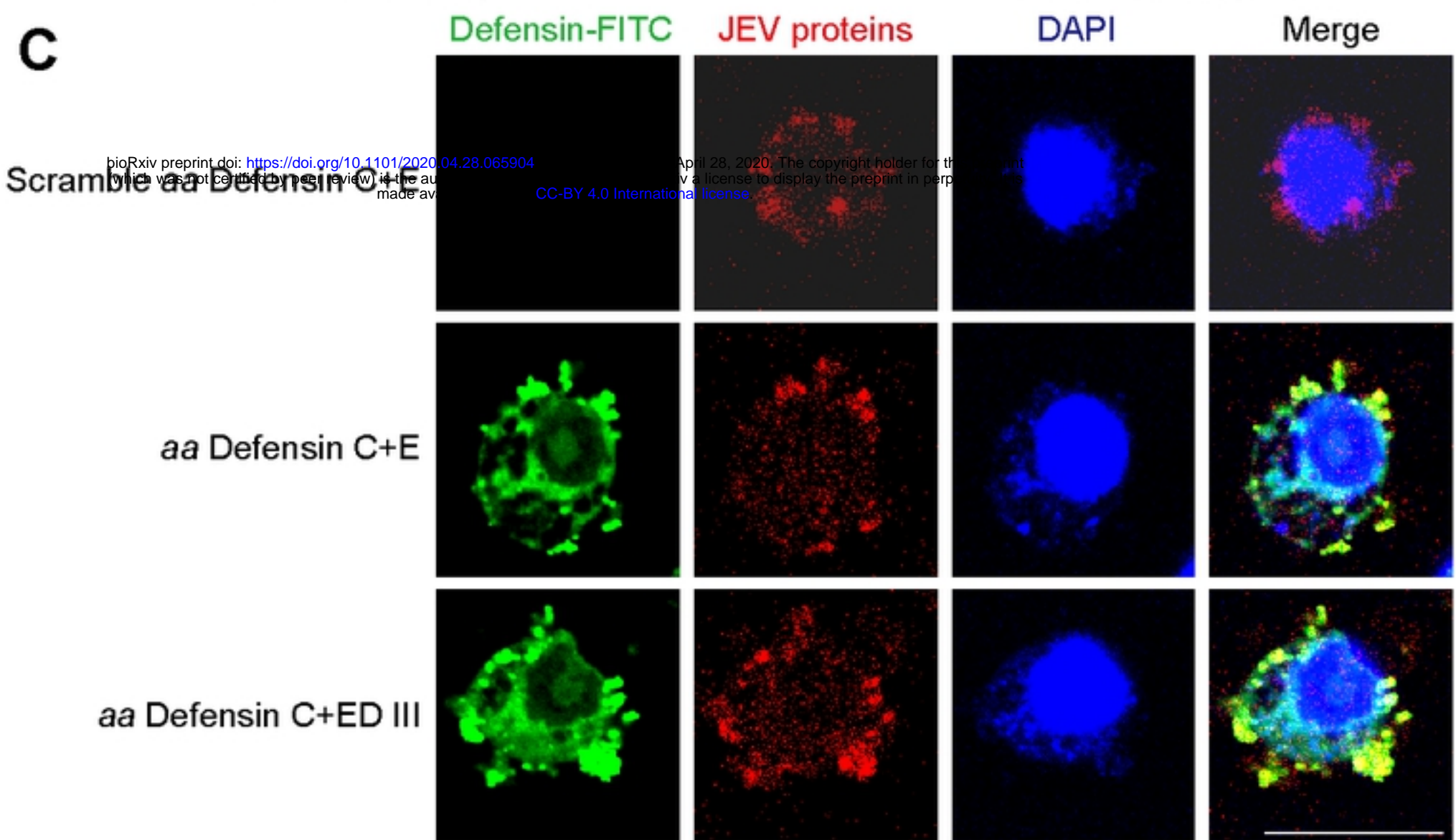
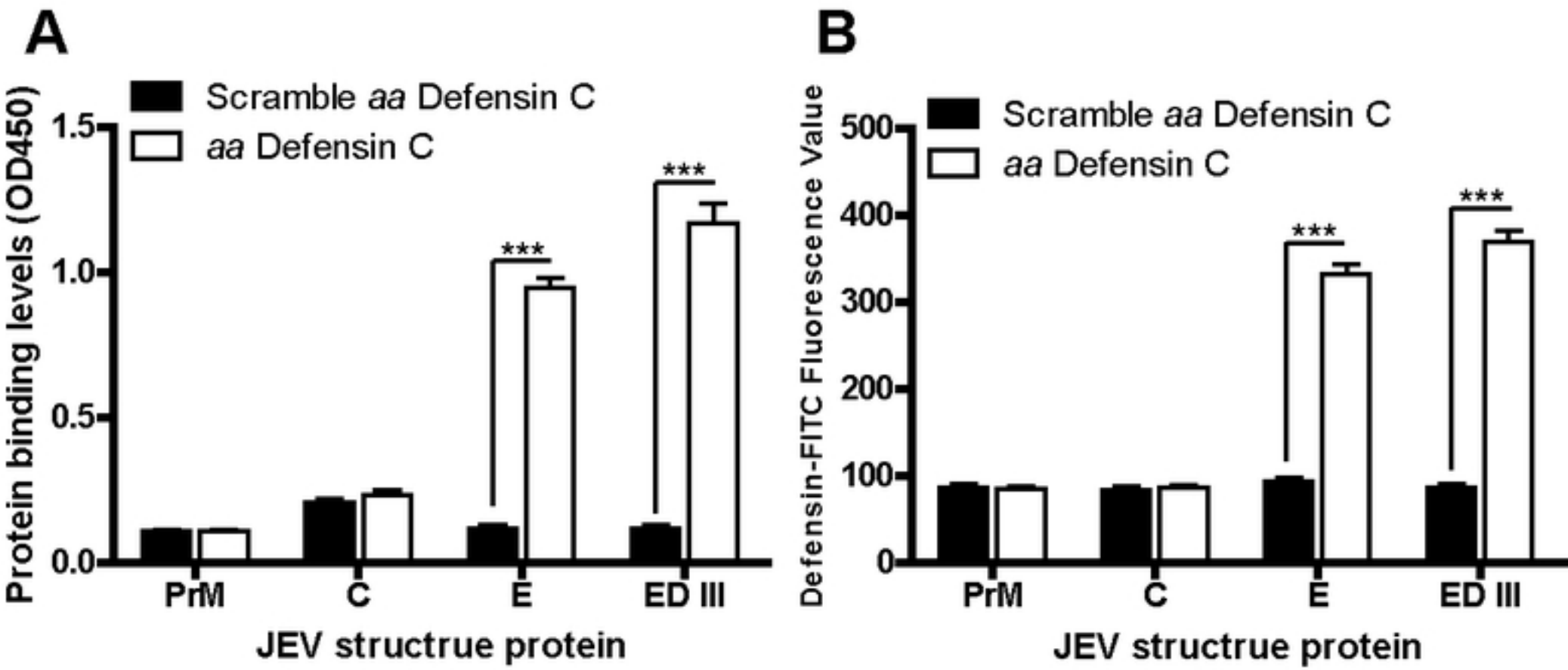


Figure 4

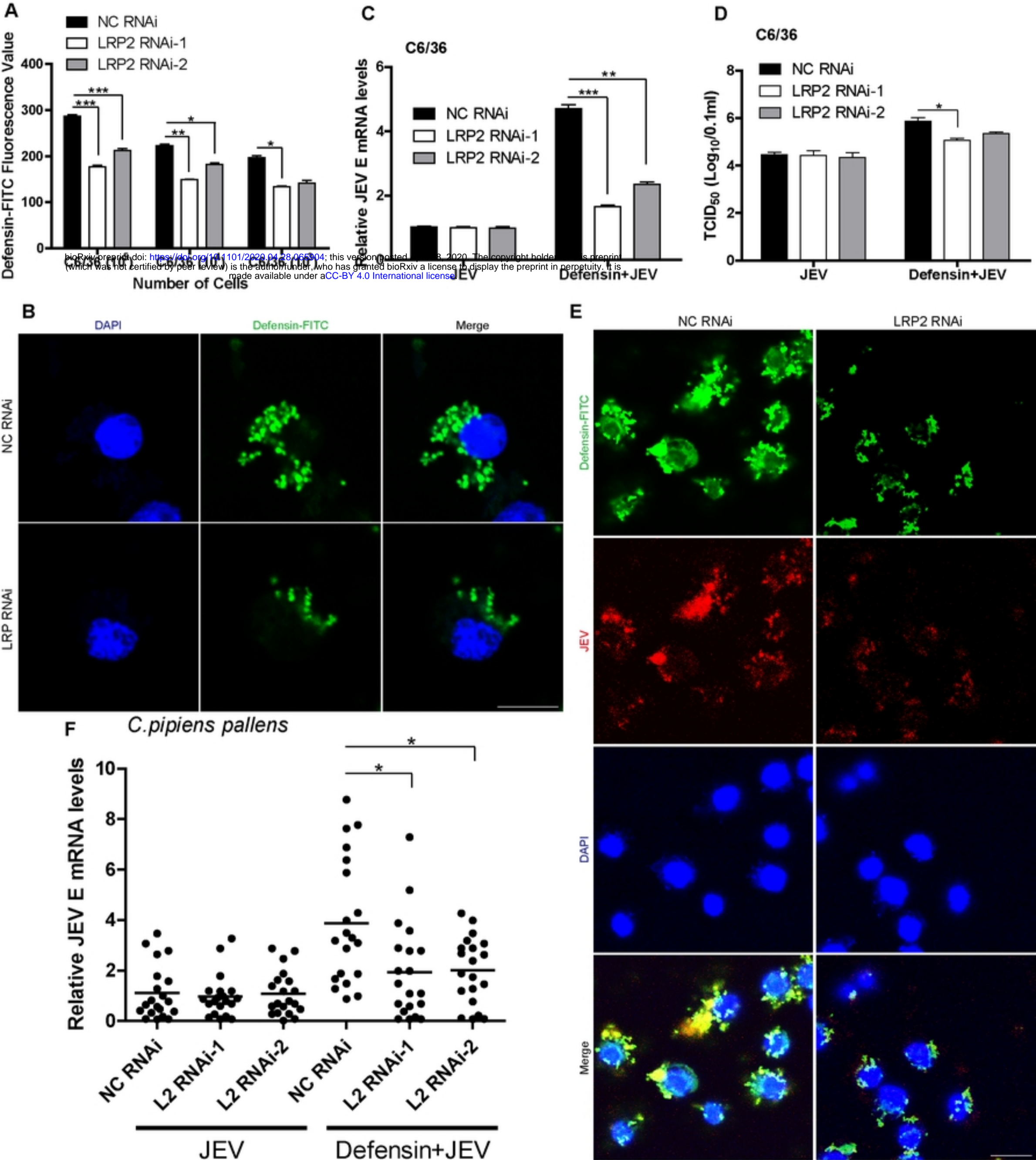
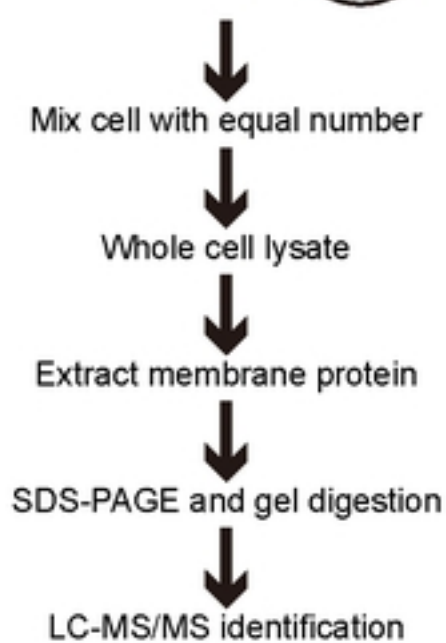
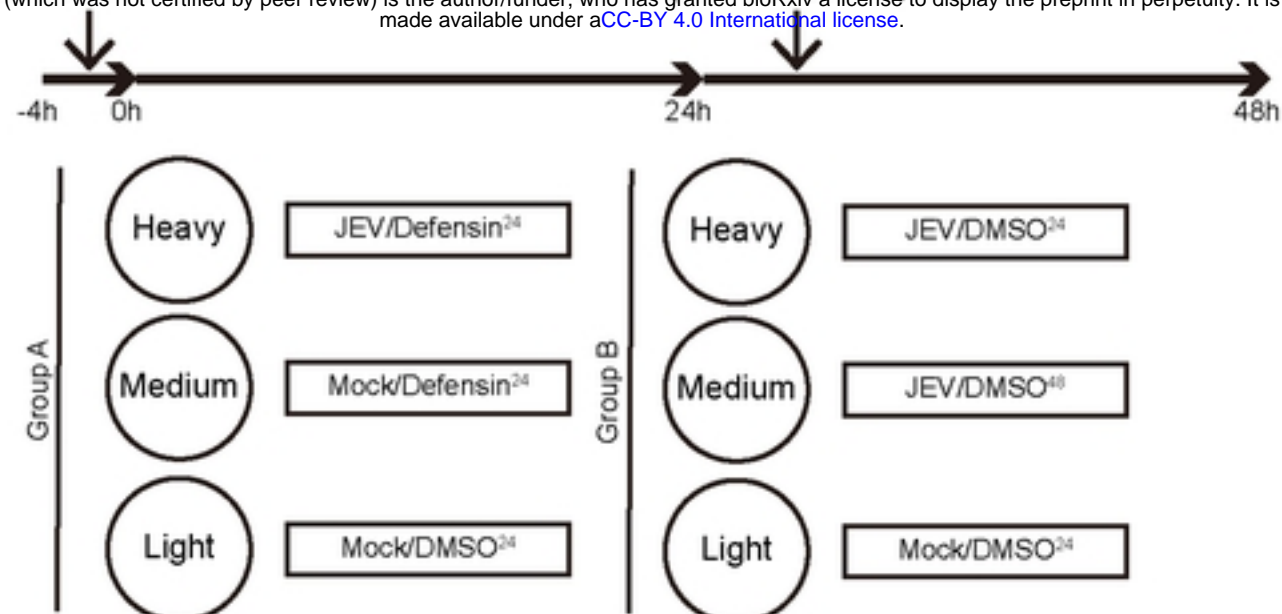


Figure 5

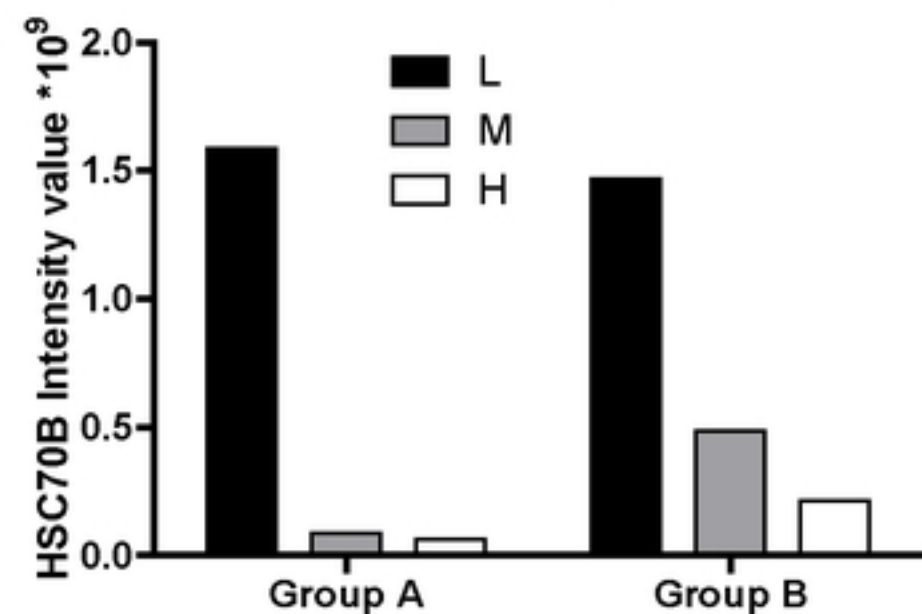
A

Mock/Virus infection at 0h for an hour. Culture with defensin (Defensin) or DMSO for 24 or 48h. bioRxiv preprint doi: <https://doi.org/10.1101/2020.04.28.065904>; this version posted April 28, 2020. The copyright holder for this preprint (which was not certified by peer review) is the author/funder, who has granted bioRxiv a license to display the preprint in perpetuity. It is made available under aCC-BY 4.0 International license.

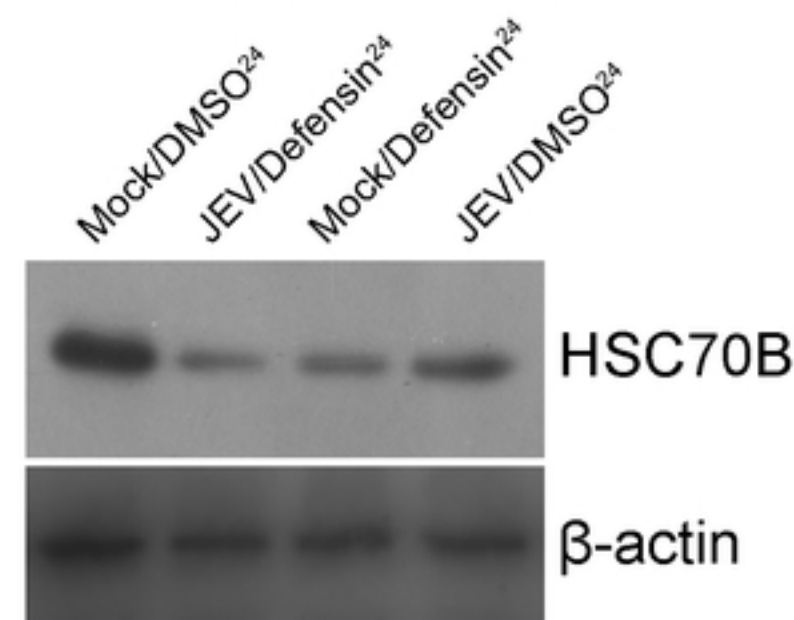


B

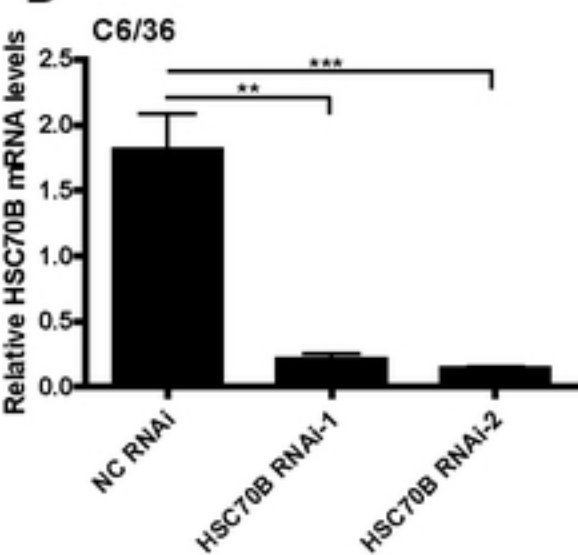
LC-MS/MS intensity



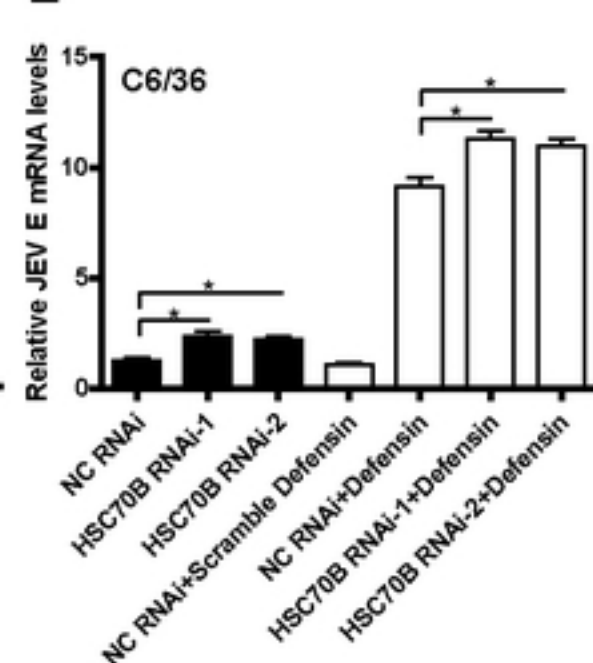
C



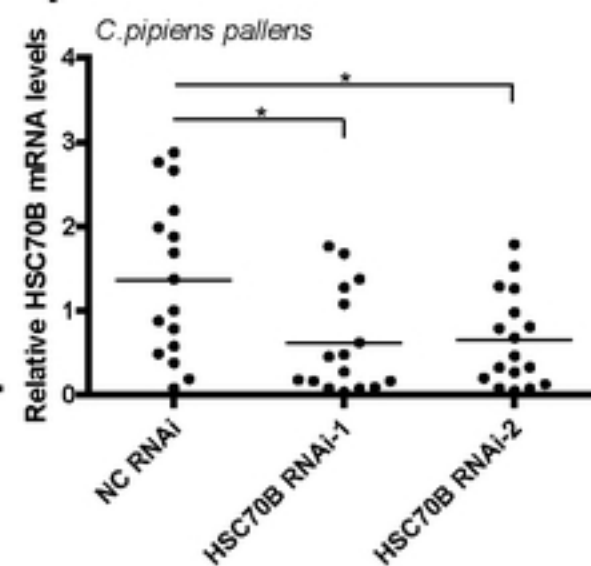
D



E



F



G

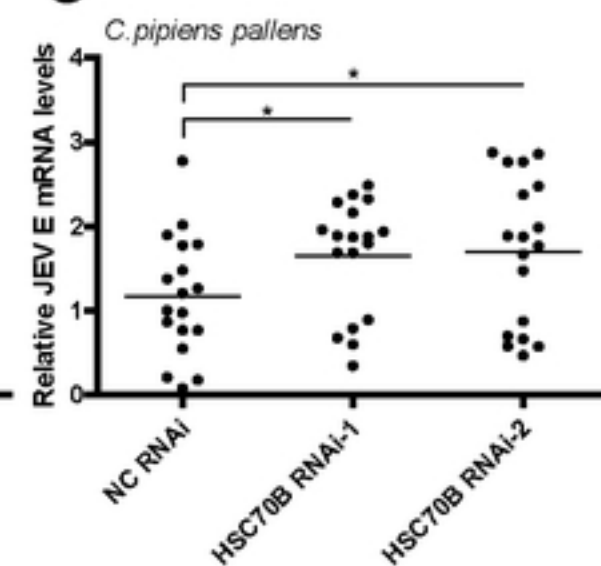


Figure 6

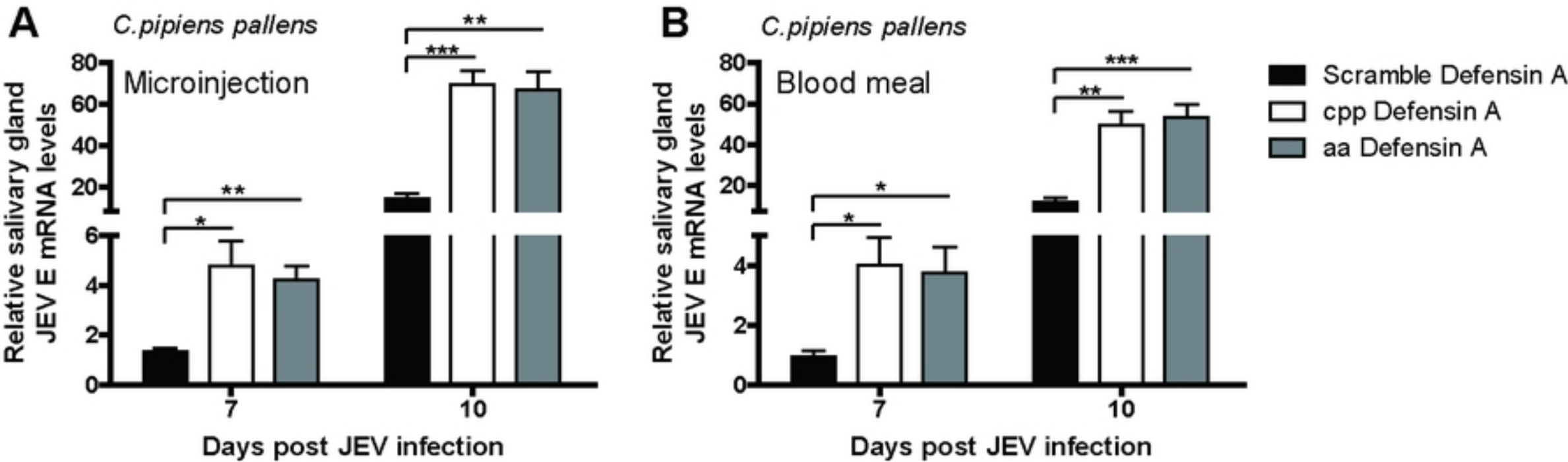


Figure 7